A. ZARGOUN

ATILIM UNIVERSITY 2021

FEEDBACK CONTROL OF SYNAPTICALLY COUPLED HODGKIN-HUXLEY NEURONS

THE GRADUATE SCHOOL OF NATURAL AND APPLIED SCIENCES
OF
ATILIM UNIVERSITY

ABOBAKAR ZARGOUN

DOCTOR OF PHILOSOPHY THESIS
IN
MODELING AND DESIGN OF ENGINEERING SYSTEMS (MAIN FIELD OF STUDY: ELECTRICAL ELECTRONICS ENGINEERING)

FEBRUARY 2021

FEEDBACK CONTROL OF SYNAPTICALLY COUPLED HODGKIN-HUXLEY NEURONS

A THESIS SUBMITTED TO
THE GRADUATE SCHOOL OF NATURAL AND APPLIED SCIENCES
OF
ATILIM UNIVERSITY

BY

ABOBAKAR ZARGOUN

IN PARTIAL FULFILLMENT OF THE REQUIREMENTS
FOR
DOCTOR OF PHILOSOPHY
IN
MODELING AND DESIGN OF ENGINEERING SYSTEMS (MAIN FIELD OF STUDY: ELECTRICAL ELECTRONICS ENGINEERING)

FEBRUARY 2021

Approval of the Graduate School of Natural and Applied Sciences, Atilim University.

_____

Prof. Dr. Ali Kara
Director

I certify that this thesis satisfies all the requirements as a thesis for the degree of **Doctor of Philosophy in Modeling and Design of Engineering Systems, Atilim University.**

_____

Prof. Dr. Ender Keskinkılıç

Head of Department

This is to certify that we have read the thesis FEEDBACK CONTROL OF SYNAPTICALLY COUPLED HODGKIN-HUXLEY NEURONS submitted by ABOBAKAR ZARGOUN and that in our opinion it is fully adequate, in scope and quality, as a thesis for the degree of Doctor of Philosophy.

_____

Prof. Dr. Reşat Özgür Doruk
Supervisor

Asst. Prof. Dr. Ali Emre Turgut
Mechanical Eng. Depart, METU _____

Prof. Dr. Reşat Özgür Doruk
Electrical and Electronics Eng. Depart, Atilim Univ. _____

Assoc. Prof. Dr. Mehmet Bulent Ozer
Mechanical Eng. Depart, METU _____

Assoc. Prof. Dr. Kemel. Efe Eseller
Electrical and Electronics Eng. Depart, Atilim Univ. _____

Asst. Prof. Dr. Yasar DALVEREN
Avionics Eng. Depart, Atilim Univ. _____

Date: 01 *February 2021*

I hereby declare that all information in this document has been obtained and presented in accordance with academic rules and ethical conduct. I also declare that, as required by these rules and conduct, I have fully cited and referenced all material and results that are not original to this work.

Abobakar, Zargoun :

Signature :

ABSTRACT

FEEDBACK CONTROL OF SYNAPTICALLY COUPLED HODGKIN-HUXLEY NEURONS

Abobakar, Zargoun

PhD., Modelling and Design of Engineering Systems

Supervisor : Prof. Dr. Reşat Özgür Doruk

February 2021, 63 pages

Through a gap junction (electrical synapse) a pair of identical Hodgkin-Huxley neuron models are coupled together. These neurons are excited by an external current. The system we have represented is a nonlinear electrical circuit and the gap is a synaptic conductance. The complete system is of nonlinear multi-input, multi-output (MIMO) type system. By using the MATLAB based software package called MATCONT and the bifurcation theory we tracked the neuron parameters that lead to bifurcation conditions. In addition, we studied the couple of the Hodgkin-Huxley model by selected different values of the synaptic conductance. For each value of the synaptic conductance we analyzed the bifurcations for the parameters of the neurons one-by-one using MATCONT. After that, we designed a controller to stabilize oscillation in the membrane potential caused by the change the parametersof the neurons. A washout filter controller of the second order type is used. This controller provides an electrical current injection to control the unwanted behaviour of the neurons due to parametric bifurcations. Linear Quadratic Regulator (LQR) supported by projective control theory, serves as the reference method in the design of the controller. The washout filter processes the membrane potentials only and projective control generates a gain to transform the filtered output to a current injection to the slave neuron.

Keywords: Hodgkin-Huxley neurons; Electrical synapses; Andronov-Hopf bifurcations; Linear quadratic regulators; Projective control.

ÖZ

SİNAPTİK OLARAK KUPLE EDİLMİŞ HODGKIN-HUXLEY NÖRONLARININ GERİ BESLEMELİ DENETİMİ

Abobakar Zargoun

Doktora., Mühendislik Sistemlerinin Modellenmesi ve Tasarımı

Tez Danışmanı: Prof. Dr. Reşat Özgür Doruk

Şubat 2021, 63 sayfa

Bir çift özdeş Hodgkin-Huxley nöron modeli, bir boşluk kavşağı (elektriksel sinaps) vasıtasıyla kuple edilmektedir. Bu nöronlar, harici bir akım tarafından uyarılırlar. Sistem doğrusal olmayan bir elektrik devresi, sinaptik boşluk ise bir elektriksel iletkenlik olarak modellenmektedir. Sistemin tamamı doğrusal olmayan çok girişli, çok çıkışlı (MIMO) bir yapı olarak karşımıza çıkar. Çatallanma teorisini ve MATLAB tabanlı MATCONT adlı paket yazılım kullanılmak suretiyle çatallanmaya yol açan nöron parametrelerini izlenmekte olup söz konusu koşullar belirlenerek kayıt altına alınmaktadır. Bu çalışmada küple edilmiş Hodgkin-Huxley modelinin parametreler, ve sinaptik iletkenliğin seçilen farklı değerleri için ayrı ayrı incelemeler yapılmıştır. Sinaptik iletkenliğin ve nöronların parametrelerinin değişik değerleri için çatallanmalar MATCONT kullanılarak incelenmiştir. Daha sonra, çatallanma olgusundan kaynaklı olduğu zar potansiyeli salınımlarını söndürmek için ikinci dereceden arındırma süzgeci tabanlı denetleyiciler kullanılmıştır. Bu denetleyici mevcut çatallanmaları kontrollü elektrik akımı uygulayarak denetim altına almaktadır. Döngünün tamamlanabilmesi için süzgeç çıkışının bir kazanç ile işlenmesi gerekmektedir. Bunun için izdüşümsel denetim yöntemi kullanılmaktadır. Bu yöntem tam durum geri beslemeli doğrusal karesel denetleyiciyi (LQR) süzgeç çıkışından geri besleme yaparak yaklaşık olarak elde etmeyi hedefler. Arındırma süzgeçleri yalnızca zar potansiyellerini işler ve izdüşümsel denetim süzgeç çıkışını bir kazanç yoluyla nörona bir akım enjeksiyonu olarak uygulanmasını sağlar.

Anahtar Kelimeler: Hodgkin-Huxley nöronları, Elektriksel sinapslar, Çatallanmalar, Arındırma Süzgeçleri, Doğrusal karesel deneleyiciler, İzdüşümsel denetim.

To my family

ACKNOWLEDGMENTS

First, I give thanks to God for protection and ability to do this work. I would like to express my special appreciation and thanks to my advisor Professor Dr. Reşat Özgür Doruk for his guidance, helpful advice and support, who made this work possible. His friendly guidance and expert advice have been invaluable throughout all stages of the work.

I would also like to thank my committee members, Assoc. Prof. Dr. Kemal Efe Eseller and Assoc. Prof. Mehmet Bulent Ozer for serving as my committee members even at hardship and for their time and valuable input. They have been a constant inspiration through their constructive criticism, insightful comments and patience.

Furthermore, my thanks are extended to the members of my examination committee.

Finally, I would like to thank my family for their support and encouragement.

TABLE OF CONTENTS

LIST OF TABLES

LIST OF FIGURES

LIST OF SYMBOLS / ABBREVIATIONS

HH	Hodgkin Huxley.
FN	Fitzhugh Nagumo.
AD	Alzheimer's Disease.
LQR	Linear Quadratic Regulator.
ODE	Ordinary Differential Equation.
PDE	Partial Differential Equation.
α	The First Lyapunov Coefficient.
σ	Parameter.
x	State Vector.
Z	State of the washout filter.
y	Measured output of the system.
I	Output of the washout filter.
u	Input to the controlled system.
n	Order of the system.
r	Number of variable feedback lines.
t	Time.
$\propto_w$	The state of the system.
β_w	The State output of the system.
J	Performance Index
A & B	Input marix in the state space representation of dynamic system.
C	Thr related matrix between the outputs of the plant and the state.
T	Nonsingulat matrix.

Λ	Diagonal eigenvalues matrix.
v	Eigenvectors matrix.
Q & R	Quadratic weight matrix.
K_f	The optimal gain.
K_0	The ouput feedback gain.
HOT	Higher Order Terms.
Gui	Graphical user interface.
MIMO	Multi Input Multi Output.
V	Membrane Potentail.#
n	The proportion of the activating molecules of the potassium channel.
m	The proportion of the activating molecules of the sodium channel.
h	The proportion of the inactivating molecules of the sodium channel.
I	External cuurent injection.
C	Membrane capacitance.
gNa	Lumped conduntance of the sodium channel.
gk	Lumped conduntance of the potassium channel.
gL	Lumped conduntance of the leakage channel.
vNa	Lumped equilibrium potentail of the sodium channel.
vK	Lumped equilibrium potentail of the potassium channel.
vL	Lumped equilibrium potentail of the leakage channel.
Gc	Conductance of the electrical synapse.

CHAPTER 1

INTRODUCTION

Most of the scientists have been worked on adapting the automatic control of dynamic systems towards solving the various problems related to the broad field of science. One of those is the field of sciences is Neuroscience. A branch (such as neurophysiology) of the life sciences that deals with the anatomy, physiology, biochemistry, or molecular biology of nerves and nervous tissue and especially with their relation to behaviour and learning. Neuroscience or neurobiology is the science which studies the nervous system and its mechanism of action [1]. Neuroscience is very important to human life. So, introducing this science under the auspices of the automatic control theory is a very important step. The human brain contains 86 billion neurons with around 19 to 23 billion neurons in the brain cortex [2]. Theneuron transfers the data signals by electrochemical mechanisms. These mechanisms depend on the different concentration of sodium (Na+), and potassium (K+) ions inside and on the membrane of the neuron. These mechanisms lead to produce a small ionic current through the neuron and small voltage potentials on the membrane of the neuron. The first modelling for biological neuron was revealed by two scholars (Hodgkin and Huxley) [3]. They put complex nonlinear high order differential equation as a model for squid giant neuron named by (F-N) model or (H.H) model. In 1961,Richard Fitzhugh put forward a new model for the neuron, who named it “Bonhoeffer-van der Pol model". After that J. Nagumo et al. created an equivalent circuit for the Fitzhugh model, to create at last the FitzhughNagumo model. Actually, they simplified the (Hodgkin and Huxley) model from the fourth order nonlinear differential equation to the second order nonlinear differential equation [4][5].

Many psychiatric and neurologic diseases, like mental retardation [6], schizophrenia [7], Parkinson's disease [8], autism [9], Alzheimer's disease (AD) [10], compulsive behaviour [11], and addiction [12] appeared because of the dysfunction in neuronal communication.

This failure in the performance of neurons was the result of problems in the synapses which connected the neurons to each other, and the critical bifurcations in the biological neuron.

Bifurcation is divided into two main types as will be seen in Chapter 3. The first one is the local bifurcation, and the second one is the global bifurcation. In local bifurcation, the perversion of a single parameter leads to the variation of the equilibrium point of the nonlinear system. So, the analysis the local bifurcation could be important in the nonlinear system theory. When the parameters of the system change the local bifurcation occurs then the stability of the system changes. There are many types of the local bifurcation like Hopf bifurcation [13.14,15,16,17] and Limit-point or Saddle-node bifurcation [13].

Another type, called the Neutral Saddle Point [14] which appears in this study is not classified as bifurcation point but, it is considered as a critical point. The last type of the bifurcation which was found was by MATCONT the Branching point or Branch point. MATCONT is a graphical MATLAB software package for the interactive numerical study of dynamical systems. MATCONT gives the ability to compute the curves of the Neutral saddle, equilibrium, limit cycles, Branch points, Hopf points, and limit points [18]. The main objective of the study is to eliminate the oscillation that occurs due to the bifurcations points which are resulted through the changes of the system parameters.

There are many methods to control the previous bifurcations points. The control methods are Linear Quadratic Regulator (LQR), Washout Filter, Projective Control Theory and Pole Placement approach. In this research, we used the washout filter controller aided by, projective control theory and the Linear Quadratic Regulator.

1.1. Aim and Scope

In this thesis we used The MATCONT toolbox software environment for analysis of the bifurcation points with MATLAB. The simulation of the coupled Hodgkin-Huxley model at the bifurcated parameters are also performed to validate the results obtained from the MATCONT software. Then, we are going to design a controller to stablize the bifurcated coupled Hodgkin-Huxley model connected together by an electrical synapse. The controller will be based on a washout filter of the second order type. The design of the washout filter will benfit from Linear Quadratic Regulator supported by Projective Control Theory. All the computaions and simulations are performed in MATLAB.

1.2. Layout of the Thesis

Chapter 1 includes the introduction, the aim of the thesis and the layout of the thesis. Chapter 2 is explaining the literature Review, introduces some of the works that have been done and, on the Hodgkin-Huxley model. Chapter 3 includes the theory and types of the bifurcations, the relationship between the bifurcations and stability in the nonlinear dynamic system. Chapter 4 study the control theory methods. Chapter 5 illustrates the Hodgkin-Huxley model, Coupled Hodgkin-Huxley model, and the bifurcation analysis by MATCONT. Chapter 6 presents the results of the washout filter controller for a Coupled Hodgkin-Huxley model. Chapter 7 Discussion and Conclusion.

CHAPTER 2

LITERARURE REVIEW

The core mathematical framework for modern biophysical neuron modelling was developed half a century ago by Sir Alan Hodgkin and Sir Andrew Huxley. They carried out an elegant series of electrophysiological experiments on the squid giant axon in the late 1940s and early 1950s[31]. The squid giant axon is notable for its extraordinarily large diameter (0.5 mm).

Most axons in the squid and other nervous systems are typically at least 100 times thinner. The large size of the squid giant axon is a specialization for rapid conduction of action potentials that trigger the contraction of the squid's mantle when escaping from a predator. In addition to being beneficial for the squid, the large diameter of the giant axon was beneficial for Hodgkin and Huxley because it permitted manipulations that were not technically feasible in smaller axons that had been used in biophysical studies up to that point. In a well designed series of experiments, Hodgkin and Huxley systematically demonstrated how the macroscopic ionic currents in the squid giant axon could be understood in terms of changes in Na+ and K+ conductances in the axon membrane. Based on a series of voltage- clamp experiments, they developed a detailed mathematical model of the voltage- dependent and time dependent properties of the Na+ and K+ conductance's. The empirical work lead to the development of a coupled set of differential equations describing the ionic basis of the action potential [28], which became known as the Hodgkin- Huxley (HH) model.

The real predictive power of th e model became evident when Hodgkin and Huxley demonstrated that numerical integration of these differential equations could accurately reproduce all the key biophysical properties of the action potential.

For this outstanding achievement, Hodgkin and Huxley were awarded the 1963 Nobel Prize in Physiology and Medicine (shared with Sir John Eccles for his work on the biophysical basis of synaptic transmission).

Electrical equivalent circuits in biophysical neural modeling, the electrical properties of a neuron are represented in terms of an electrical equivalent circuit. Capacitors are used to model the charge storage capacity of the cell membrane, resistors are used to model the various types of ion channels embedded in membrane, and voltage sources are used to represent the electrochemical potentials established by varying intra- and extracellular ion concentrations. In their seminal paper on the biophysical basis of the action potential [29], modelled a segment of squid giant axon using an equivalent circuit similar to that shown in Figure 2.1.

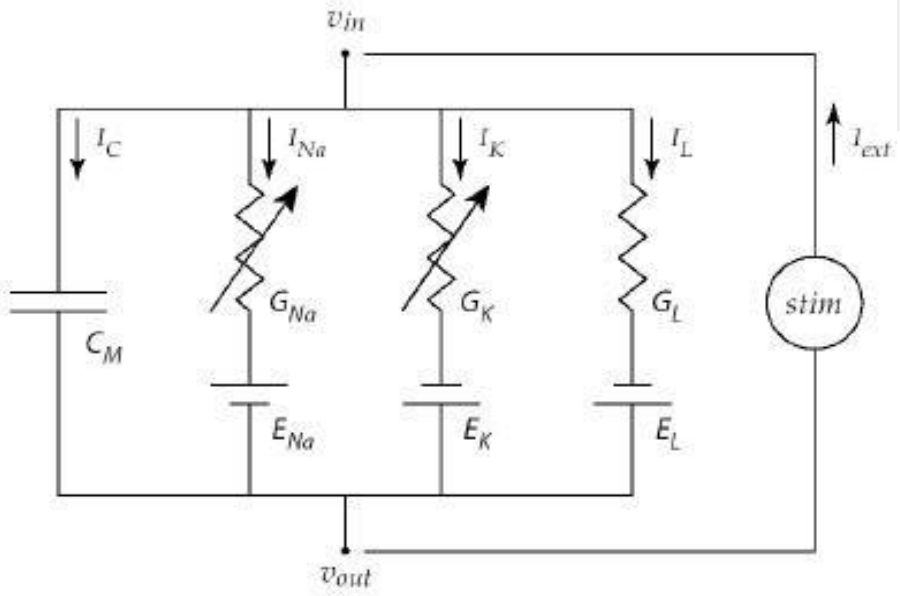

Figure 2. 1 Electrical equivalent circuit for a short segment of squid giant axon

In the equivalent circuit, the current across the membrane has two major components, one associated with the membrane capacitance and one associated with the flow of ions through resistive membrane channels.

The basic mathematical structure of the modern neural cell model was developed by Alan Lloyd Hodgkin who graduated from the University of Cambridge and Andrew Fielding Huxley who graduated from Westminster school in London more than sixty years ago [1]. A series of electrical experiments from years 1940 to 1950 on the nerve of an Atlantic giant squid's axon was carried out by them. The axon of the

giant squid was characterized by a huge diameter nearly of (0.5 mm), which was larger than the most axons in other Organisms by 100 times. The large diameter of the giant axon was beneficial to Hodgkin and Huxley because it allowed the manipulations that were technically impossible in the small axons used in biophysical studies up to that point. They got a nonlinear differential equation and computational complex neuron model for the biological model of neuron known as Hodgkin-Huxley model. By a series of clamp voltage experiments Hodgkin and Huxley systematically explained how one could understand the micro-ionic currents in the giant squid axon in the series of changes through the density of (K+ and Na+) behavior in the axon membrane (action potential) or (voltage-clamp) which was a constant electrical potential applied to a neuron membrane in order to measure the ionic currents [3]. The Hodgkin and Huxley model were very important because it was symbolized by the behavior of a genuine neuron. By this model, they were awarded the Nobel Prize [1][3]. After that, several scholars worked to simplify it. So that, a group of models could appear.

2.1. Physical Meaning

Most of what we think of as our mental life involves the activities of the nervous system, especially the brain. This nervous system is composed of billions of cells, the most essential being the nerve cells or neurons. There are estimated to be as many as 100 billion neurons in our nervous system! A typical neuron has all the parts that any cell would have, and a few specialized structures that set it apart. The main portion of the cell is called the soma or cell body. It contains the nucleus, which in turn contains the genetic material in the form of chromosomes. Neurons have many extensions called dendrites. They often look likes branches or spikes extending out from the cell body. It is primarily the surfaces of the dendrites that receive chemical messages from other neurons [34].

One extension is different from all the others and is called the axon. Although in some neurons, it is hard to distinguish from the dendrites, in others it is easily distinguished by its length. The purpose of the axon is to transmit an electro-chemical signal to other neurons.

At the very end of the axon is the axon ending, which goes by a variety of names such as the bouton, the synaptic knob, the axon foot, and so on. It is there that the electro-chemical signal that has travelled the length of the axon is converted into a chemical message that travels to the next neuron.

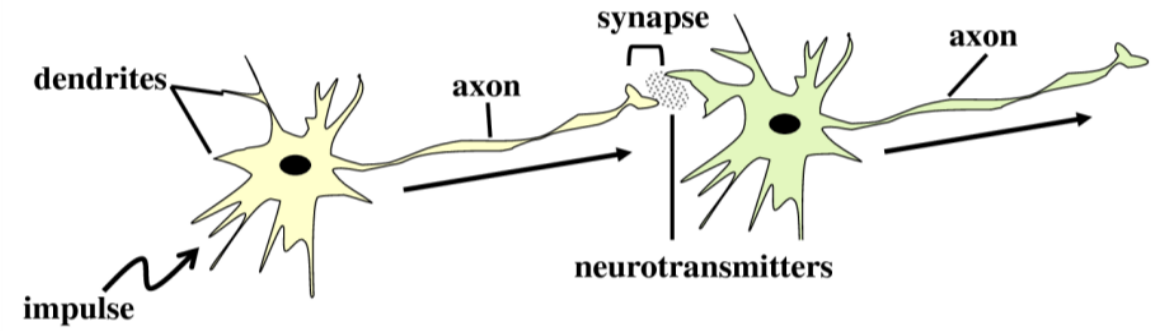

Figure 2. 2 Structure of Neuron

CHAPTER 3

BIFURCATION THEORY

The splitting of the main body into two parts refers to the bifurcation phenomena. Bifurcation problems may have important implications in biological systems. Henri Poincaré, a French mathematician who was the first person to invent the name “Bifurcation”. He used this term in 1885 in his mathematics paper showing this behavior [22]. The bifurcation theory is the study of changes in the qualitative structure mathematically by varying parameters of the dynamica system. So that, any small smooth change in a system parameter produce a sudden "qualitative" or topological change in its behavior and therefore, the bifurcation occurs. Bifurcation has a negative effect on the physical systems because of the high-amplitude oscillations or instability. In the continuous systems like: (ODEs or PDEs) and discrete systems, the bifurcations appear. In biological models, the bifurcation is relative to the characteristics of the equilibrium points which has specific change.

3.1. Types of Bifurcation

There are two types of bifurcations. Local bifurcation and Global bifurcation. The main field of concentration for this research is the Local bifurcation

3.1.1 Local Bifurcation

The local bifurcation is the bifurcation which can be fully analyzed with the changes in the characteristics of the local stability of equilibrium point. It occurs when a parameter’s change causes the stability of an equilibrium point to change [23]. The local bifurcation is more interesting in engineering problems. So that, we are going to focus on the local bifurcations. There are several types of local bifurcation.

3.1.2. Global Bifurcation

Global bifurcations occur when 'larger' invariant sets, such as periodic orbits, collide with equilibria. This causes changes in the topology of the trajectories in the phase space which cannot be confined to a small neighborhood, as is the case with local bifurcations. We are concentrating on local Bifurcation only.

3.1.1.1 Saddle-Node Bifurcation

The Saddle-Node is one of the types of local bifurcation. It is basically a collide of two converging equilibriums or two fixed points of a dynamical system and annihilates each other. The collision leads to annihilate of the equilibrium in a dynamical system. This bifurcation is characterized by a single zero eigenvalue in the Jacobean of the system. This type of bifurcation has many names like tangential bifurcation, fold bifurcation and blue skies bifurcation. The Saddle-Node name can be referenced to continuous dynamical systems, but the fold bifurcation name can be referenced to the discrete dynamical systems. A differential equation below which represents an example of a saddle-node bifurcation [25]:

$$\dot{m}(t) = s + m^2$$

where

m is the variable of the state, and (s) is the parameter of the bifurcation at fixed point

$$\dot{m}(t) = 0$$

So,

$s + m^2 = 0$

where

$m = \pm\sqrt{-s}$

Therefore, the fixed point exists only at $s \leq 0$, and when $s > 0$, we have imaginary fixed point. If ($s > 0$) the equilibrium points do not exist. If $s < 0$ two equilibrium points exist, one of them is stable at $-\sqrt{-s}$ which can be located at the left side of the $\dot{x}$ axis, the other one is unstable at $+\sqrt{-s}$ because it is at the right side of the $\dot{m}$ axis.

If $(s = 0)$, the bifurcation point exists, in this case, there will be one equilibrium which points only. The fixed point will be called saddle-node fixed point and it is will not hyperbolic. The stable fixed point collides with the unstable fixed point and after that it will disappear.

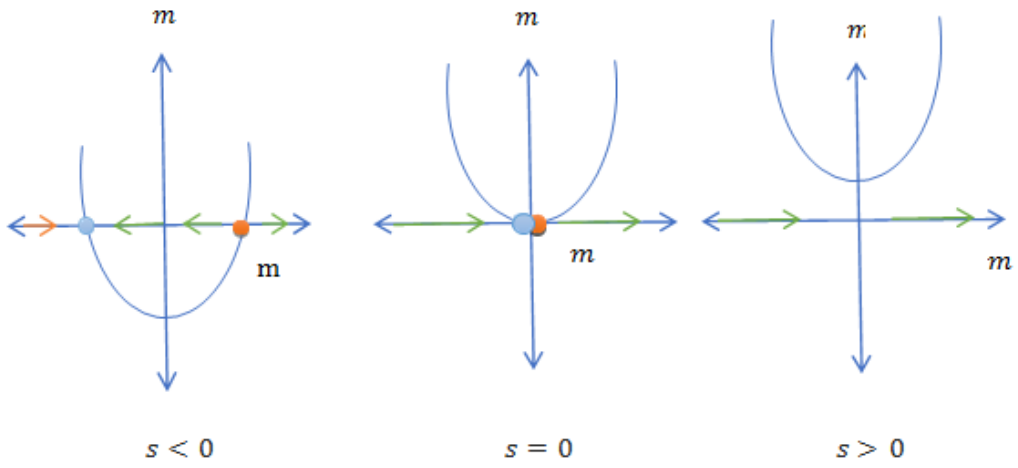

Figure 3. 1 The Saddle-Node Bifurcation

3.1.1.2 Neutral Saddle Point

Neutral saddle points are not classified as bifurcations but considered as critical points. The stability of the equilibrium leading to a Neutral Saddle is lost due to a pair of real value eigenvalues that are equal in magnitude and opposite in signs.

3.1.1.3 Branch-Point Bifurcation

The branch point, can be two equilibrium path branches emit so there is no individual tangent . The branch-point bifurcation appear when the real part of the eigenvalue crosses zero.

3.1.1.4 Hopf Bifurcation

Henri Poincaré, Eberhard Hopf, and Aleksandra Andronov [17]. When a periodic solution or limit cycle appears and the system's stability switches, the critical point,

in this case, represents the Hopf-bifurcation. In another word, the Hopf-bifurcation is a tool to prove the existence of limit cycles. Where limit cycle is a periodical oscillation that is stable to perturbations. Mentioned scientists analyzed the bifurcation in the two dimensional plane when the limit cycle erupts from the equilibrium point. This phenomenon can be characterized by a pair of pure complex conjugate eigenvalues in the Jacobian of the system. The critical of the Hopf Bifurcation determines the quality of limit cycle. Therefore, there are two types of Hopf bifurcation the first is supercritical and the second is subcritical. When the Hopf bifurcation case is Supercritical and a specific quantity which called the first Lyapunov coefficient is negative so this erupts the limit cycle which is stable. In other cases, the erupts limit cycle will be unstable which yields the subcritical bifurcation.

The general form of a Hopf bifurcation is:

$$\frac{dH}{dt} = H((\sigma + i) + b|H|^2$$

where H and b are complex and σ is a parameter. So,

$$b = \propto + j\beta$$

α : the first Lyapunov coefficient.

The limit cycle is stable when $\propto$ is negative and $\sigma > 0$

$$H(t) = re^{jwt}$$

Where $r = \sqrt{\frac{-\sigma}{\alpha}}$ and $w = 1 + \beta r^2$

Then the bifurcation is called supercritical.

The limit cycle is unstable when $\propto$ is positive and $\sigma > 0$. Then the bifurcation is called subcritical.

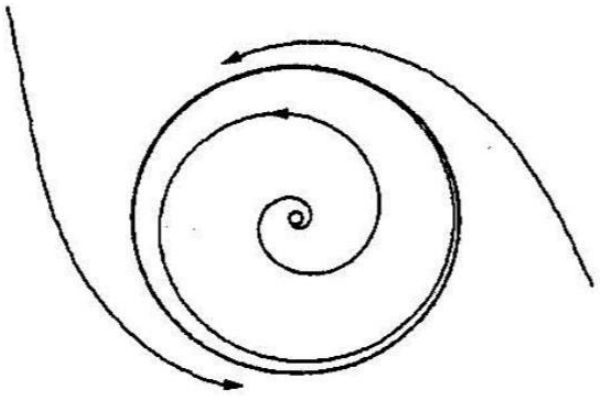

Figure 3. 2 Supercritical Hopf bifurcation when α is negative and $\sigma > 0$.

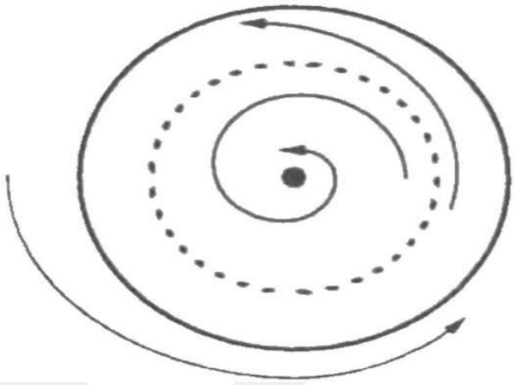

Figure 3. 3 Subcritical Hopf bifurcation when α is positive and $\sigma < 0$

3.2. Equilibrium Point

Consider a differential equation represent a nonlinear system.

$$\dot{x}(t) = f\,(x(t), u(t))$$

If there is a specific input $(\bar{u} \in R^m)$ which called the equilibrium input. A point $(\bar{x} \in R^n)$ is called an equilibrium point where (f) is the function mapping of $(R^n * R^m \rightarrow R^n)$. For example, assume $\bar{x}$ is an equilibrium point with equilibrium input $(\bar{u})$ and the system is $f(\bar{x}, \bar{u})$. So, when the system $\dot{x}(t) = f\,(x(t), u(t))$ starting from initial condition $x(t_0) = \bar{x}$, and the input is $u(t) = \bar{u}$ for all $t \geq t_0$.

The resulting solution $x(t)$) satisfies $x(t)$= $x(t) = \bar{x}$ for all $t \geq t_0$. As a result, it is called an equilibrium point.

3.3. Nonlinear Dynamic System

When a system's output is not proportional to its inputs the system is called a nonlinear system [24]. Engineers, physicists, mathematicians and scientists are very interested in Nonlinear system problems [25]. This is because most systems in nature are nonlinear. The general form of a nonlinear system can be written as:

$$\dot{X} = f\ (x, u, t)$$

$$\dot{Y} = g\ (x, u, t)$$

The above system has input signal which is (u). Therefore, the system without input signal will be as shown below.

$$\dot{X} = f\ (x\ , t)$$

$$\dot{Y} = g\ (x, t)$$

Where

x : is state vector, $x \in R^n$

u : is input or control signal, $u \in R$ y: is output, $y \in R^r$

n : is the order of the system

r : is the number of available feedback lines.

3.4. Linearization

Nonlinear differential equations represent most of the governing real-life processes. When one encounter a problem of the nonlinear type it is very difficult to analyze it by mathematical methods unless one makes some changes to the nonlinear equation. So, there will a need to simplify the nonlinear equation in order to obtain a solvable equation in the usual math methods. For this purpose, one will use the Linearization methods which is based on Tayler series expansion. For example: Let us assume the nonlinear system as

$$\dot{x}(t)\ =\ f\ (x(t), u(t))$$

Let (x_0, u_0) is an equilibrium point, that is (x_0, u_0) =0

One can expand the functions (x, u) around (x_0, u_0) by using Taylor Series, as:

$$f\ (x,u) = f\ (x_0\ , u_0) + \frac{df}{dx}(x_0, u_0) * (x\ , x_0) + \frac{df}{du}(x_0\ , u_0) * (u\ , u_0) + H.O.T$$

$H.O.T$ is a Higher Order Terms in Taylor Series expansion. If one omits the $H.O.T$ the equation will represent the approximate behavior of the nonlinear system near $(x_0\ , u_0)$.

Where

$$f\ (x_0\ ) = 0$$

So,

$$\dot{x}(t) = f(x)\ = f\ (x_0\ ) + \frac{df}{dx}(x\ -\ x_0) = \frac{df}{dx}(x\ -\ x_0) = \frac{df}{dx}\delta x$$

The variation of the trajectories x_0 is $\delta x = x\ -\ x_0$

The $\dot{x}_0$ is a constant So,

$\delta x = \dot{x}\ -\ \dot{x}_0 = \dot{x}$

$(x_0\ , u_0)$ point represent the equilibrium point. So that $f\ (x_0\ , u_0) = 0$. Then

$$\dot{x}(t) = f\ (x_0\ , u_0) + \frac{df}{dx}(x_0, u_0) * (x - x_0) + \frac{df}{du}(x_0\ , u_0) * (u\ -\ u_0)$$

$$\delta\dot{x} = \frac{df}{dx}(x_0, u_0) * (x - x_0) + \frac{df}{du}(x_0\ , u_0) * (u - \ u_0)$$

From the last equation, we can form a linear system as:

$$[\dot{x}(t)] = \left[\frac{df}{dx}(x_0, u_0) \qquad \frac{df}{du}(x_0\ , u_0)\right]\begin{bmatrix}\delta x \\ \delta u\end{bmatrix}$$

$$[\dot{x}(t)] = A\ (x\ -\ x_0) + B\ (u\ -\ u_0)$$

Then

$$A = \frac{df}{dx} \quad , \quad B = \frac{df}{du}$$

A and B are matrices which are called Jacobian matrices at (x_0, u_0). From the Jacobian matrix A one can find the eigenvalues of the system, which can be determined by the nature of the solution nearly equilibrium point , as:

1. If the Jacobian matrix produces an eigenvalues with the negative real part, it means the original system has a locally stable equilibrium point.
2. If the Jacobian matrix produces an eigenvalues with the positive real part, it means the original system has a locally unstable equilibrium point.

3.5. MATCONT Software

MATCONT is a graphical MATLAB software package for the interactive numerical study of dynamical systems. It allows to compute curves of equilibria, limit points, Hopf points, limit cycles, period doubling bifurcation points of limit cycles, fold, flip and torus bifurcation points of limit cycles [20].

The MATCONT gui makes the standard MATLAB ODE Suite interactively available and provides computational and visualization tools. MATCONT uses the MATLAB symbolic toolbox whenever it is available; higher order derivatives are important example in the computation of normal forms.

The sparsity of the discretized systems for the computation of limit cycles and their bifurcation points is exploited by using the standard MATLAB sparse matrix methods.

The MATLAB software package MATCONT provides an interactive environment for the continuation and normal form analysis of dynamical systems. This analysis is complementary to the simulation of the systems which is also included in the package and can be used in their identification, control, and optimization.

MATCONT is designed to exploit the power of MATLAB. It is developed in parallel with the continuation toolbox MATCONT, a package of MATLAB routines that can be used from the command line.

CHAPTER 4

THEORITICAL METHODS OF CONTROL

4.1. Linear Quadratic Regulater

Optimal controllers are the best possible controllers especially in Multi Input Multi Output (MIMO) control system designs, the optimal control can be a very handy tool in control law derivation. A fast and practical method to derive linear control gains is the linear quadrature regulator.

This method is better than pole placement method in terms of the ability to compute the state feedback control gain matrix in a systematic way [27],[28].

One will assume the linear model to be controlled by an optimal regulator is given by the equation as shown below.

$$\dot{x} = Ax + Bu \qquad (4.1)$$

In the optimal control approach, we will have a linear control gain matrix (K):

$$u(t) = -Kx(t) \qquad (4.2)$$

This equation is optimal for any initial state $x(0)$, one can minimize the performance index by.

$$J = \int_0^\infty (x^T Q x + u^T R u) dt \qquad (4.3)$$

where

Q : positive definite or positive-semi-definite.

R : positive definite.

The matrices Q and R determine the importance of the error and the expenditure of energy which accounts for $(u^T Ru)$.

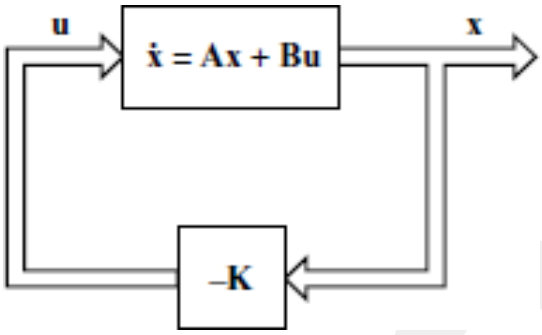

Figure 4. 1 Linear Quadratic Regulator Block Diagram

One will solve the optimization problem. Substituting equation (4.2) into equation (4.3), It gets.

$$\dot{x} = Ax - BKx = (A - BK)x \qquad (4.4)$$

suppose the matrix $A - BK$ is stable, or this matrix has negative real parts eigenvalues. Substituting equation (4.2) into (4.3) equation, one shall get.

$$J = \int_0^\infty (x^T Qx + x^T K^T RKx)dt \qquad (4.5)$$

$$J = \int_0^\infty x^T (Q + x^T K^T RK)xdt \qquad (4.6)$$

Let us make

$$x^T (Q + x^T K^T RK)x = -\frac{d}{dt}(x^T Px) \qquad (4.7)$$

P matrix is a positive definite or real symmetric. Yields

$$x^T (Q + x^T K^T RK)x = -\dot{x}^T Px - x^T P\dot{x} = -x^T [(A - BK)^T P + P(A - BK)]x \qquad (4.8)$$

The equation (4.8) has to be true for any (x) after comparing the two sides of this equation. So that

$$(A - BK)^T P + P(A - BK) = -(Q + K^T RK) \qquad (4.9)$$

The matrix (P) is a positive definite when one approves $(A - BK)$ is stable, and the matrix (P) will satisfy the equation (4.9). So, one will need to see if the matrix (P) is positive definite after determining this matrix from equation (4.9). When the system is stable the matrix (P) will not be unique which may satisfy the equation (4.9). Therefore, if one finds one (P) matrix positive definite for this equation and the system is stable, then one must cancel other (P) matrices which is not positive

definite. One can find the performance index as shown below:

$$J = \int_0^\infty x^T(Q + K^T RK)xdt = -x^T Px\,|_0^\infty = -x^T(\infty)Px(\infty) + x^T(0)Px(0) \quad (4.10)$$

Assume all eigenvalues of $A - BK$ has negative real parts, so $x(\infty) \to 0$ and the result is

$$J = x^T(0)Px(0) \quad (4.11)$$

From this term include (P) matrix and initial condition $x(0)$ we can find the performance index J.

matrix is positive definite or real symmetric matrix for quadratic optimal control problem.

$$Q = T^T * T \quad (4.12)$$

T is a nonsingular matrix. So, we can rewrite the equation (4.9) as

$$(A^T - K^T B^T)P + P(A - BK) + Q + K^T T^T TK = 0 \quad (4.13)$$

Or

$$A^T P + PA + [TK - (T^T)^{-1}B^T P]^T[TK - (T^T)^{-1}B^T P] - PBR^{-1}B^T P + Q = 0 \quad (4.14)$$

The minimization of the equation (4.15) is a requirement of minimizing the J equation with respect to K.

$$x^T[TK - (T^T)^{-1}B^T P]^T[TK - (T^T)^{-1}B^T P]x \quad (4.15)$$

The last equation is not negative. So, when it is zero the minimum happens, or in case

$$TK = (T^T)^{-1}B^T P \quad (4.16)$$

And therefore,

$$K = T^{-1}(T^T)^{-1}B^T P = R^{-1}B^T P \quad (4.17)$$

Hence

One can find the optimal matrix K from equation (4.17). So, the optimal control law is

$$u(t) = -Kx(t) = -R^{-1}B^T P * x(t) \quad (4.18)$$

The equation (4.9) must be satisfied by the P matrix of the equation (4.17).

$$A^T P + PA - PBR^{-1}B^T P + Q = 0 \quad (4.19)$$

The equation (4.19) called Riccati equation or reduced matrix. The design steps are

1. Solve the Riccati equation for P matrix. The system or matrix $A - BK$ is stable when the P matrix is positive definite.
2. Find the optimal matrix K by substitute P matrix in equation (4.17).

4.2. Washout Filter Theory

The Washout filter acts as a high pass filter which only allows the transient part of the input signal and it helps to keep the natural equilibrium points in the physical nonlinear system without change. The represented form of the washout filter on s-domain is as [32].

$$G(s) = \frac{Y(s)}{X(s)} = \frac{s}{(s+a)}$$

$$G(s) * (s+a) = s$$

$$G(s) * s + G(s) * a = s$$

$$G(s) = 1 - \frac{a}{s+a}$$

The high-pass-filter can be represented in state-space as:

$$z = \propto_w z + \beta_w y$$

$$I = \propto_w z + \beta_w y$$

Where

z: State of the washout filter $z \in R^n$.

y: Measured output of the system.

I: Output of the washout filter and it is the input (u) to the controlled system $I \in R$.

$\propto_w$: is the state of the system $\propto_w \in R^{r*c}$. r is a row, c is a column.

β_w : State of the output of the system $\beta_w \in R^r$.

The number of columns in β_w depends on the size of (y). To apply the state feedback control techniques, one must have to augment the washout filter to the original nonlinear system. $\propto_w$ must be Hurwitz matrix or stable matrix which mean all eigenvalues of this matrix have negative real part.

4.3. Projective Control Theory

The projective control method which is a linear method is used in the approximation of state feedback. Here the state feedback can be obtained by whatever method such as (L.Q.R). One cannot retain all the eigenvalues of the state feedback system when using projective control method. The number of available outputs for feedback determines the number of retainable eigenvalues. In the application, the optimal control matrix (K_f) which is obtained from the state feedback is the reference for the projective control method.

Assume the system as shown below

$$\dot{x} = Ax + Bu$$
$$y = Cx$$

Where

x: State of linear plant $(x \in R^n)$.

u: Input of the linear plant $(u \in R^m)$.

y: Output which feed the feedback$(y \in R^r)$.

A: $(A \in R^{n*n})$

B: $(B \in R^{n*m})$

C: Related matrix between the outputs of the plant and the state $(C \in R^{n*r})$. r is available feedback lines.

The full state feedback control signal defined as below

$$u = -K_f x$$

The gain matrix $(K_f \in R^{m*n})$ is the matrix which obtained by using (L.Q.R) theory.
The close loop of state feedback is

$$\dot{x} = A - BK_f x$$

The eigen spectrum of closed loop of state feedback determine as showed below

$$\Lambda = \begin{bmatrix} \lambda I & \dots & 0 \\ \vdots & \ddots & \vdots \\ 0 & \dots & \lambda n \end{bmatrix}, v = [v_1, v_2 \ \dots\dots, v_n]$$

$$\Lambda = \text{eig}(A - BK_f)$$

Λ: Diagonal eigenvalues matrix.

v: Eigenvectors matrix.

The Eigen spectrum equation is:

$$A - BK_f v = \Lambda v$$

The control signal u obtained

$$u = -K_0 y$$

Where

$$y = Cx$$

So

$u = -K_0 Cx$

The closed-loop dynamic of the output feedback can be found as:

$$\dot{x} = (A - BK_0 C)x$$
$$(A - BK_0 C)v_r = v_r \Lambda_r$$
$$\left(A - BK_f\right)v_r = (A - BK_0 C)v_r$$

From the last equation, we can find the relationship between K_f & K_0

$K_0 = K_f v_r (C v_r)^{-1}$

The output feedback gain is K_0.

CHAPTER 5

COUPLED HODGKIN-HUXLEY MODEL

5.1. The Single Hodgkin-Huxley Model

The traditional Hodgkin-Huxley model in [28] is a highly nonlinear 4th order model aiming at the quantitative description of a single neuron membrane or more truly speaking, the giant axon of the European squid. It includes the dynamical properties of the membrane potential and the permeabilities of the sodium, potassium and leakage (mainly chloride) ion channels. That also has one external input which represents the current due to a possible stimulus or a test input (voltage clamp etc.). One can define it mathematically as:

$$C\frac{dv}{dt} = I_{ext} - g_{Na}m^3h(v - v_{Na}) - g_K n^4(v - v_K - g_L(v - v_L)$$

$$\frac{dm}{dt} = a_m(v)(1 - m) - \beta_m(v)m$$

$$\frac{dn}{dt} = a_n(v)(1 - n) - \beta_n(v)n \qquad (5.1)$$

$$\frac{dh}{dt} = a_h(v)(1 - h) - \beta_h(v)h$$

where v is the membrane potential in mV, m and h are the activation and inactivation variables of the sodium channel respectively and n is the activation of the potassium channel. The variables m, n, h are dimensionless and varies in the range [0, 1]. The model can be externally stimulated by an input current represented by I_{ext}. In the above equation there are also three conductance parameters g_{Na}, g_K and g_L which represents the lumped conductance of sodium, potassium and leakage channels respectively. In addition all channels have an equilibrium potential that are represented by vNa, vK and vL for sodium, potassium and leakage channels respectively. aj and bj are nonlinear functions in sigmoidal forms,

As we are interested in the coupled Hodgkin-Huxley equations, the details together with the synaptic coupling will be discussed in the next section.

5.2. The Coupled Hodgkin-Huxley Model

In this work, we are dealing with a coupled neural model formed by synoptically coupling two identical Hodgkin-Huxley neurons. Here, the synapse is represented by an electrical conductance gc and the coupling is performed through electrical current inputs. As a result, one can express the coupled Hodgkin-Huxley equations as:

$$C_1\frac{dv_1}{dt} = I_1 - g_{Na1}m_1^3h_1(v_1 - v_{Na}) - g_{K1}n_1^4(v_1 - v_K) - g_{L1}(v_1 - v_L) - g_c(v_1 - v_2)$$

$$C_2\frac{dv_2}{dt} = I_2 - g_{Na2}m_2^3h_2(v_2 - v_{Na}) - g_{K2}n_2^4(v_2 - v_K) - g_{L2}(v_2 - v_L) - g_c(v_2 - v_1)$$

$$\frac{dm_1}{dt} = a_m(v_1)(1 - m_1) - \beta_m(v_1)m_1$$

$$\frac{dm_2}{dt} = a_m(v_2)(1 - m_1) - \beta_m(v_2)m_2$$

$$\frac{dn_1}{dt} = a_n(v_1)(1 - n_1) - \beta_n(v_1)n_1 \qquad (5.2)$$

$$\frac{dn_2}{dt} = a_n(v_2)(1 - n_2) - \beta_n(v_2)n_2$$

$$\frac{dh_1}{dt} = a_h(v_1)(1 - h_1) - \beta_h(v_1)h_1$$

$$\frac{dh_2}{dt} = a_h(v_2)(1 - h_2) - \beta_h(v_2)h_2$$

Where,

$$a_n(v_i) = \frac{0.1 - 0.01v_i}{\exp(1 - 0.1v_i) - 1}$$

$$a_m(v_i) = \frac{2.5 - 0.01v_i}{\exp(2.5 - 0.1v_i) - 1}$$

$$a_h(v_i) = 0.07\exp\left\{\frac{-v_i}{20}\right\}$$

$$\beta_n(v_i) = 0.125exp\left\{\frac{-v_i}{80}\right\} \quad (3)$$

$$\beta_m(v_i) = 4exp\left\{\frac{-v_i}{18}\right\}$$

$$\beta_h(v_i) = \frac{1}{\exp(3 - 0.1v_i) + 1}$$

The definitions of the state variables in (5.2) can be seen in **Table 5.1**.The definitions of the physical parameters and their nominal values are available in **Table 5.2.**

Table 5. 1 The definitions and units of the state variables and inputs in (2)

Variable Difnition Unit	**Variable Difnition Unit**	**Variable Difnition Unit**
v1	The membrane potential of the master neuron	**mV**
v2	The membrane potential of the slave neuron	**mV**
m1	Represents the proportion of the activating molecules of the sodium channels on the membrane of the master neuron	Dimensionless and varies between 0 and 1
m2	Represents the proportion of the activating molecules of the sodium channels on the membrane of the slave neuron	Dimensionless and varies between 0 and 1
n1	Represents the proportion of the activating molecules of the potassium	Dimensionless and varies

	channels on the membrane of the master neuron	between 0 and 1
n2	Represents the proportion of the activating molecules of the potassium channels on themembrane of the slave neuron	Dimensionless and varies between 0 and 1
h1	Represents the proportion of the inactivating molecules of the sodium channels on the membrane of the master neuron	Dimensionless and varies between 0 and 1
h2	Represents the proportion of the inactivating molecules of the sodium channels on the membrane of the slave neuron	Dimensionless and varies between 0 and 1
I1	External current injection to master neuron	µA/cm^2
I2	External current injection to slave neuron	µA/cm

Table 5. 2 The definitions and units of the state variables and inputs in (2)

Variable	Definition	Value	Unit
C_1	Membrane capacitance of the master neuron	0.91	mS/cm^2
C_2	Membrane capacitance of the slave neuron	0.91	mS/cm^2
g_{Na1}	Lumped conductance of the sodium channels of the master neuron	120	mS/cm^2
g_{Na2}	Lumped conductance of the sodium channels of the slave neuron	120	mS/cm^2
g_{K1}	Lumped conductance of the potassium channels of the master neuron	36	mS/cm^2
g_{K2}	Lumped conductance of the potassium channels of the slave	36	mS/cm^2

	neuron		
g_{L1}	Lumped conductance of the leakage channels of the master neuron	0.3	mS/cm^2
g_{L2}	Lumped conductance of the leakage channels of the slave neuron	0.3	mS/cm^2
v_{Na1}	Lumped equilibrium potential of the sodium channels of the master neuron	115	mV
v_{Na2}	Lumped equilibrium potential of the sodium channels of the slave neuron	115	mV
v_{K1}	Lumped equilibrium potential of the potassium channels of the master neuron	-12	mV
v_{K2}	Lumped equilibrium potential of the potassium channels of the slave neuron	-12	mV
v_{L1}	Lumped equilibrium potential of the leakage channels of the master neuron	10.6	mV
v_{L2}	Lumped equilibrium potential of the leakage channels of the slave neuron	10.6	mV
g_c	Conductance of the electrical synapse	0.3 (varied)	mS

In **Figures 5.1** and **5.2**, one can see a typical response pattern of the model in (**5.2**) with nominal parameters in **Table 5.2.**

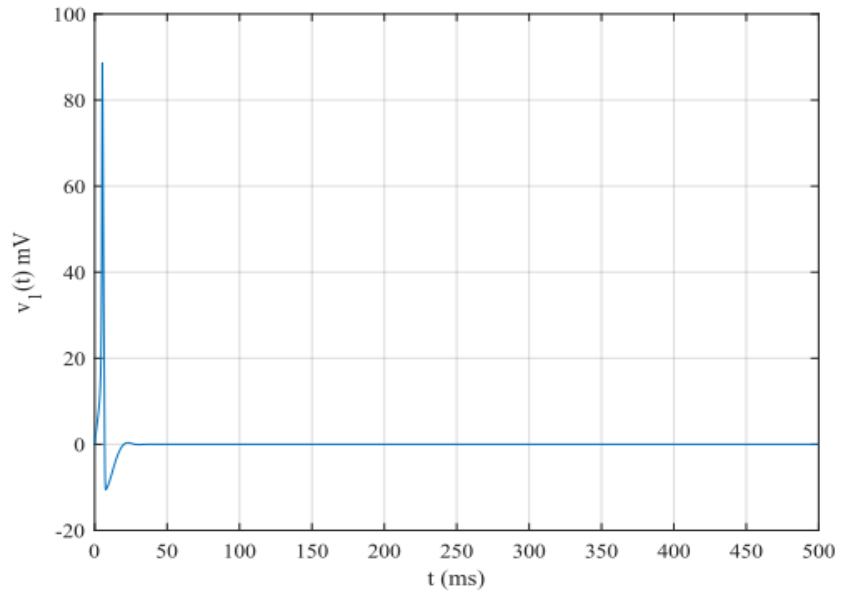

Figure 5. 1 A typical response of the model in (5.2) with nominal parameters in Table 5.2

Here, the inputs are $I_1 = 0$ and $I_2 = 0$. This is the membrane potential of the master neuron $v_1(t)$

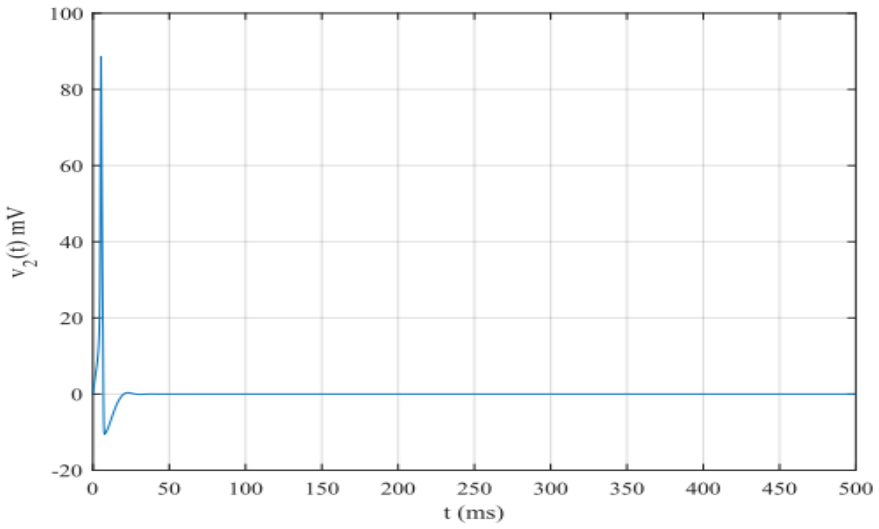

Figure 5. 2 A typical response of the model in (5.2) with nominal parameters in Table 5.2. Here, the inputs are I1 = 0 and I2 = 0. This is the membrane potential of the master neuron v2(t).

5.3. Bifurcation analysis results

Starting the MATCONT continuer using the bellow as the initial condition some points are found As the Saddle and Hopf bifurcations. The following results are found by tracing over the potassium or sodium channel conductance. In the following tables, the bifurcation points found by MATCONT software are presented.

Table 5. 3 Bifurcation analysis results for gK1 when gc = 0.3

Parameters	gk=36, gna=120, gl=0.3, Vk=-12, Vna=115, Vl=10.6, Cm=0.91				
Equilibrium points	gk1=15.4	gk1=10.7	gk1=9.59	gk1=9.67	gk1=8.09
	V1=3.29	V1=6.13	V1=10.5	V1=14.2	V1=23.0
	V2=0.65	V2=1.16	V2=1.89	V2=2.46	V2=3.67
	n1=0.37	n1=0.41	n1=0.48	n1=0.54	n1=0.65
	m1=0.08	m1=0.11	m1=0.16	m1=0.23	m1=0.45
	h1=0.48	h1=0.38	h1=0.24	h1=0.17	h1=0.06
	n2=0.33	n2= 0.34	n2=0.35	n2=0.36	n2=0.38
	m2=0.06	m2=0.06	m2=0.07	m2=0.07	m2=0.08
	h2=0.57	h2=0.55	h2=0.53	h2=0.51	h2=0.47
Type of condition	Hopf	Hopf	Limit Point	Limit Point	Natural Saddle
Equilibrium points	gk1=6.99	gk1=3.38	gk1=0.07	gk1=0.55	gk1=0.54
	V1=25.9	V1=35.1	V1=54.3	V1=102	V1=173
	V2=4.02	V2=5.05	V2=6.85	V2=10.1	V2=13.3
	n1=0.69	n1=0.77	n1=0.88	n1=0.96	n1=0.99
	m1=0.52	m1=0.74	m1=0.94	m1=0.99	m1=0.99
	h1=0.06	h1=0.02	h1=0.01	h1=0.01	h1=0.01
	n2=0.38	n2=0.39	n2=0.43	n2=0.48	n2=0.53
	m2=0.08	m2=0.09	m2=0.11	m2=0.16	m2=0.22
	h2=0.45	h2=0.42	h2=0.36	h2=0.26	h2=0.18
Type of condition	Hopf	Hopf	Hopf	Limit Point	Limit Point

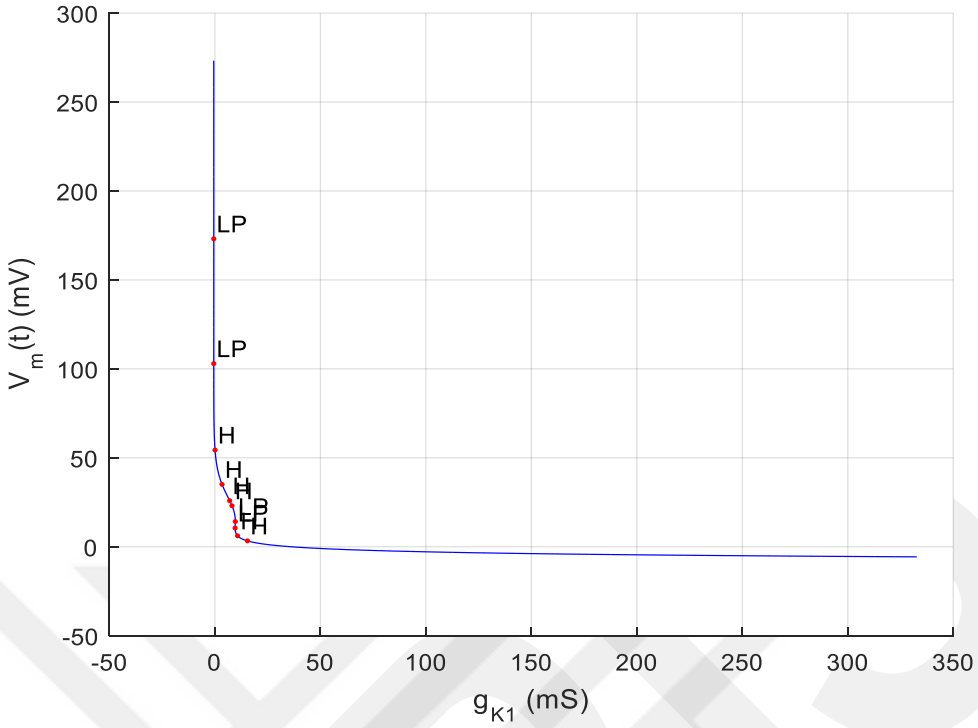

Figure 5. 3 Bifurcation diagram of H-H model against varying parameter gK1 when gc=0.3 in Table 5.3

Table 5. 4 Bifurcation analysis results for gnal when gc = 0.3

Parameters	gk=36, gna=120, gl=0.3, Vk=-12, Vna=115, Vl=10.6, Cm=0.91				
Equilibrium points	gna1=242	gna1=344	gna1=348	gna1=396	gna1=388
	V1=1.13	V1=2.95	V1=3.06	V1=7.37	V1=13.2
	V2=0.23	V2=0.58	V2=0.61	V2=1.38	V2=2.31
	n1=0.34	n1=0.36	n1=0.37	n1=0.43	n1=0.52
	m1=0.06	m1=0.07	m1=0.075	m1=0.12	m1=0.21
	h1=0.56	h1=0.49	h1=0.49	h1=0.34	h1=0.19
	n2=0.32	n2=0.33	n2=0.33	n2=0.34	n2=0.35
	m2=0.05	m2=0.06	m2=0.06	m2=0.06	m2=0.07
	h2=0.59	h2=0.58	h2=0.57	h2=0.55	h2=0.51
Type of condition	Hopf	Neutral saddle	Hopf	Limit Point	Limit Point

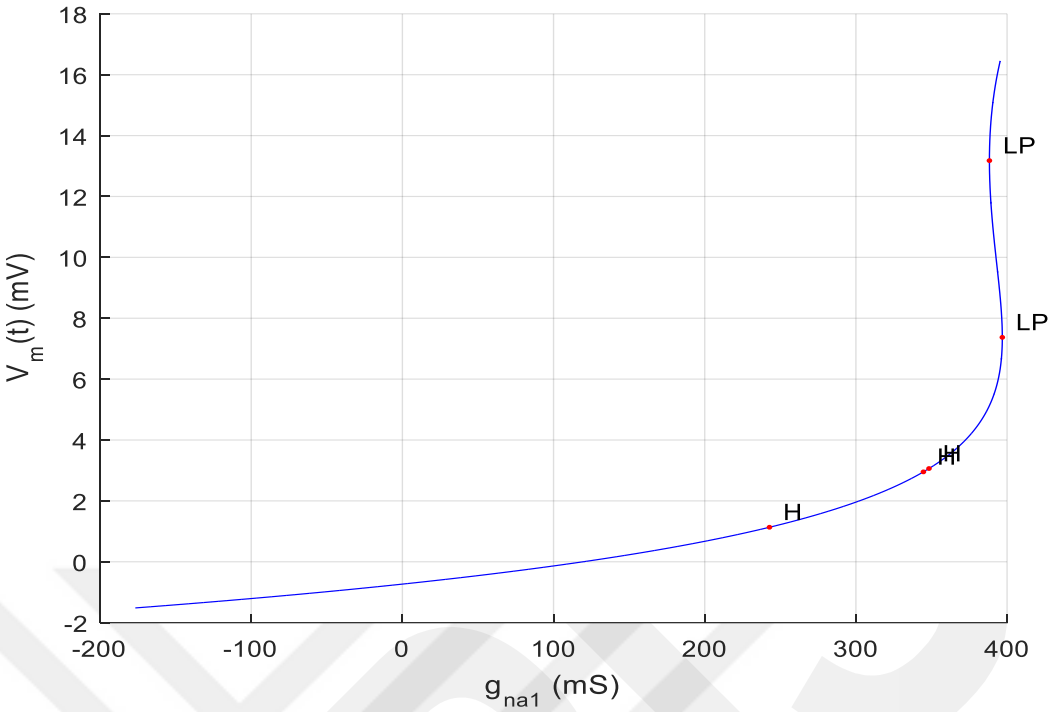

Figure 5. 4 Bifurcation diagram of H-H model against varying parameter gnal when gc=0.3 in Table 5.4.

Table 5. 5 Bifurcation analysis results for gK1 when gc = 0.55

Parameters	gk=36, gna=120, gl=0.3, Vk=-12, Vna=115, Vl=10.6, Cm=0.91				
Equilibrium points	gk1=15.4	gk1=10.8	gk1=9.59	gk1=9.67	gk1=8.10
	V1=3.29	V1=6.14	V1=10.5	V1=14.2	V1=23.0
	V2=0.65	V2=1.17	V2=1.89	V2=2.46	V2=3.67
	n1=0.37	n1=0.41	n1=0.48	n1=0.54	n1=0.66
	m1=0.08	m1=0.11	m1=0.17	m1=0.23	m1=0.45
	h1=0.48	h1=0.38	h1=0.25	h1=0.17	h1=0.06
	n2=0.33	n2= 0.34	n2=0.35	n2=0.36	n2=0.38
	m2=0.06	m2=0.06	m2=0.07	m2=0.07	m2=0.08
	h2=0.57	h2=0.55	h2=0.53	h2=0.51	h2=0.47
Type of condition	Hopf	Hopf	Limit Point	Limit Point	Hopf

Equilibrium points	gk1=6.99	gk1=3.38	gk1=0.07	gk1=0.5	gk1=0.54
	V1=25.9	V1=35.0	V1=54.4	V1=103	V1=173
	V2=4.02	V2=5.05	V2=6.85	V2=10.1	V2=13.3
	n1=0.69	n1=0.77	n1=0.88	n1=0.96	n1=0.99
	m1=0.52	m1=0.74	m1=0.94	m1=0.99	m1=1.11
	h1=0.05	h1=0.02	h1=0.01	h1=0.01	h1=0.01
	n2=0.38	n2=0.40	n2=0.43	n2=0.48	n2=0.52
	m2=0.08	m2=0.09	m2=0.11	m2=0.16	m2=0.22
	h2=0.45	h2=0.42	h2=0.36	h2=0.26	h2=0.18
Type of condition	Hopf	Hopf	Hopf	Limit Point	Limit Point

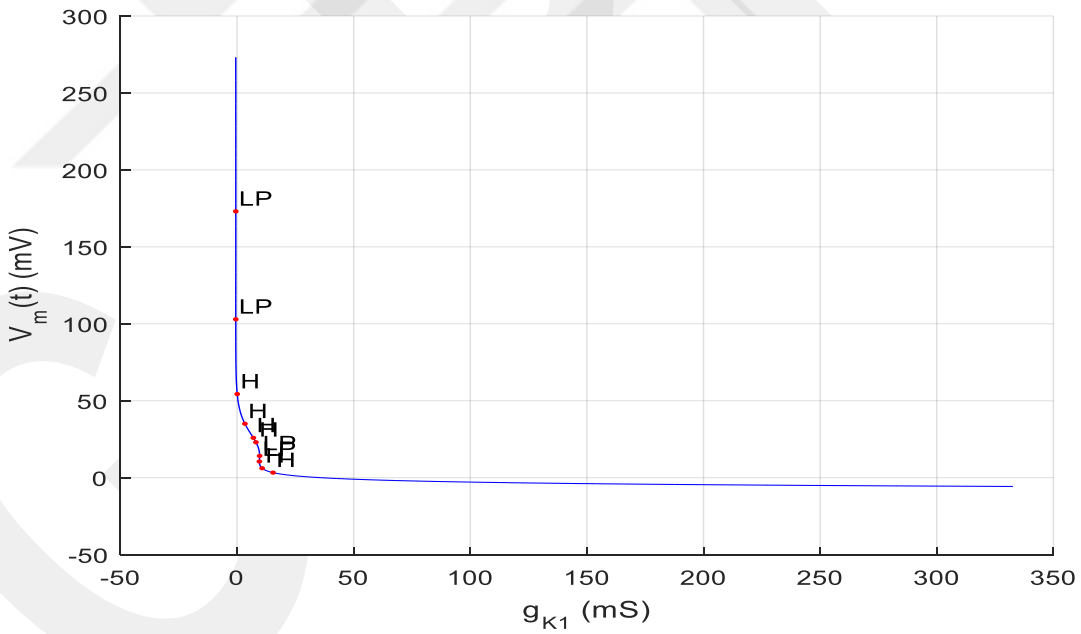

Figure 5. 5 Bifurcation diagram of H-H model against varying parameter gK1 when gc=0.55 in Table 5.5.

Table 5. 6 Bifurcation analysis results for gnal when gc = 0.55

Parameters	gk=36, gna=120, gl=0.3, Vk=-12, Vna=115, Vl=10.6, Cm=0.91			
Equilibrium points	gna1=255	gna1=363	gna1=367	gna1=414
	V1 = 1.15	V1 = 2.96	V1 = 3.07	V1 = 6.93
	V2 = 0.36	V2 = 0.91	V2 = 0.94	V2 = 1.98
	n1 = 0.34	n 1 = 0.36	n1 = 0.37	n1 = 0.43
	m1 = 0.06	m1 = 0.07	m1 = 0.08	m1 = 0.12
	h1 = 0.56	h1 = 0.49	h1 = 0.48	h1 = 0.35
	n2 = 0.32	n2 = 0.33	n2 = 0.33	n2 = 0.35
	m2 = 0.06	m2 = 0.06	m2 = 0.06	m2 = 0.067
	h2 = 0.58	h2 = 0.56	h2 = 0.56	h2 = 0.53
Type of condition	Hopf	Neutral saddle	Hopf	Limit Point

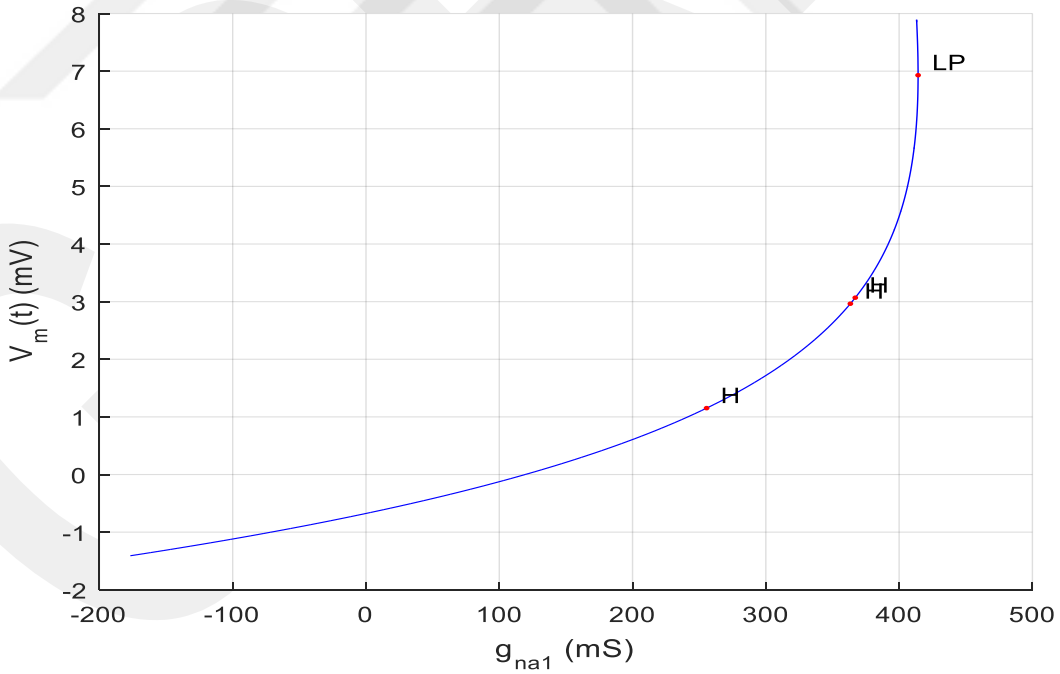

Figure 5. 6 Bifurcation diagram of H-H model against varying parameter gnal when gc=0.55 in Table 5.6.

Table 5. 7 Bifurcation analysis results for gK1 when gc = 1

Parameters	gk=36, gna=120, gl=0.3, Vk=-12, Vna=115, Vl=10.6, Cm=0.91			
Equilibrium points	gk1 = 11.2	gk1=6.14	gk1 = 7.41	gk1 = 6.19
	V1=3.42	V1=8.41	V1=17.3	V1=24.3
	V2=1.48	V2=3.32	V2=5.93	V2=7.56
	n1=0.37	n1=0.45	n1=0.58	n1=0.67
	m1=0.079	m1=0.13	m1=0.30	m1=0.48
	h1=0.47	h1=0.31	h1=0.12	h1=0.05
	n2=0.34	n2=0.37	n2=0.41	n2=0.44
	m2=0.06	m2=0.08	m2=0.10	m2=0.12
	h2=0.54	h2=0.48	h2=0.39	h2=0.33
Type of condition	Hopf	Limit Point	Limit Point	Hopf
Equilibrium points	gk1 = 5.43	gk1 = 1.14	gk1 = 1.12	gk1 = 1.12
	V1=26.5	V1=2.42	V1=149	V1=51.5
	V2=8.03	V2=16.4	V2=20.4	V2=20.6
	n1=0.69	n1=0.95	n1=0.98	n1=0.99
	m1=0.54	m1=0.99	m1=1.10	m1=1.11
	h1=0.04	h1=0.01	h1=0.01	h1=0.01
	n2=0.44	n2=0.57	n2=0.62	n2=0.63
	m2=0.13	m2=0.28	m2=0.38	m2=0.39
	h2=0.32	h2=0.13	h2=0.08	h2=0.08
Type of condition	Hopf	Limit Point	Hopf	Limit Point

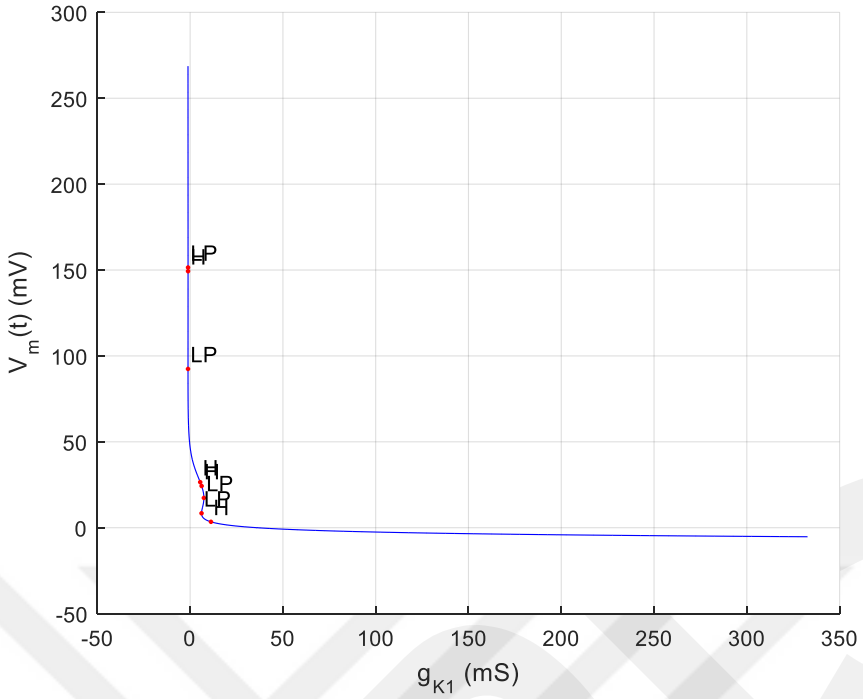

Figure 5. 7 Bifurcation diagram of H-H model against varying parameter gK1 when gc=1 in Table 5.7.

Table 5. 8Bifurcation analysis results for gnal when gc = 1

Parameters	gk=36, gna=120, gl=0.3, Vk=-12, Vna=115, Vl=10.6, Cm=0.91				
Equilibrium points	gna1 = 268	gna1 = 375	gna1 = 387	gna1 = 390.	gna1 = 408
	V1=1.14	V1=2.69	V1=2.96	V1=3.06	V1=3.64
	V2=0.51	V2=1.18	V2=1.29	V2=1.33	V2=1.57
	n1=0.33	n1=0.36	n1=0.36	n1=0.37	n1=0.37
	m1=0.06	m1=0.07	m1=0.07	m1=0.08	m1=0.08
	h1=0.56	h1=0.50	h1=0.49	h1=0.49	h1=0.47
	n2=0.33	n2=0.34	n2=0.34	n2=0.34	n2=0.34
	m2=0.06	m2=0.06	m2=0.06	m2=0.06	m2=0.06
	h2=0.58	h2=0.55	h2=0.55	h2=0.55	h2=0.54
Type of condition	Hopf	Hopf	Hopf	Hopf	Hopf

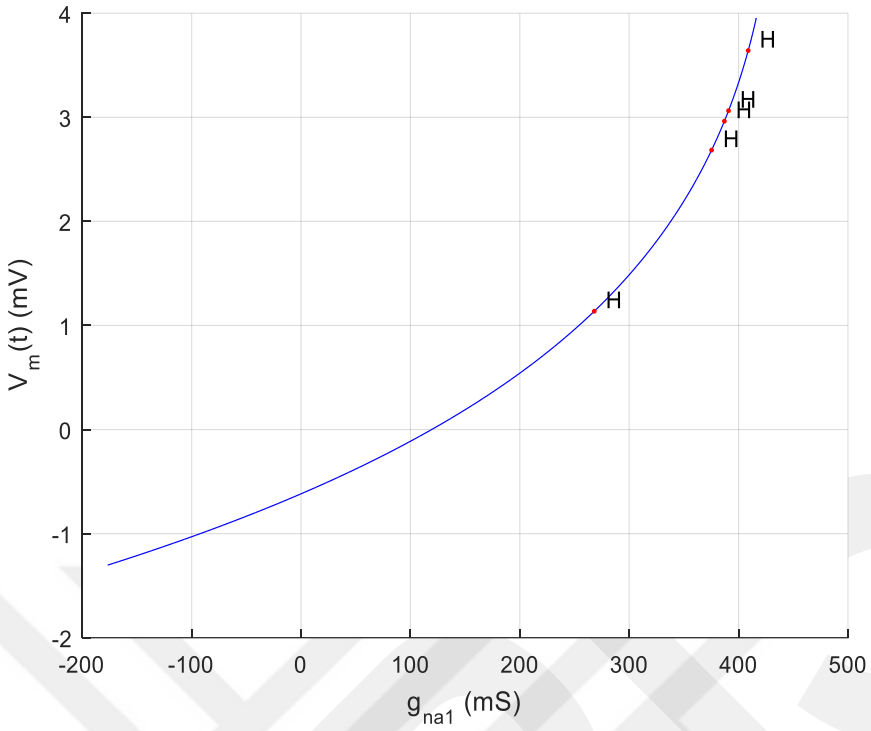

Figure 5. 8 Bifurcation diagram of H-H model against varying parameter gnal when gc=1 in Table 5.8.

Table 5. 9 Bifurcation analysis results for gK1 when gc = 10

Parameters	gk=36, gna=120, gl=0.3, Vk=-12, Vna=115, Vl=10.6, Cm=0.91			
Equilibrium points	gk1 = 5.34	gk1 = 3.59	gk1 = 3.67	gk1 = 5.16
	V1=2.89	V1=5.80	V1=5.86	V1=8.63
	V2= 2.52	V2=4.93	V2=4.98	V2=7.12
	n1=0.36	n1=0.41	n1=0.41	n1=0.45
	m1=0.074	m1=0.10	m1=0.10	m1=0.14
	h1=0.49	h1=0.39	h1=0.39	h1=0.30
	n2=0.36	n2=0.40	n2=0.40	n2=0.43
	m2=0.07	m2=0.09	m2=0.09	m2=0.12
	h2=0.51	h2=0.42	h2=0.42	h2=0.35
Type of condition	Hopf	Hopf	Hopf	Limit Point
	gk1 = 3.26	gk1 = 1.84	gk1 = 3.01	gk1 = 6.40
	V1=14.5	V1=21.3	V1=29.1	V1=51.3

Equilibrium points	V2=11.1	V2=15.1	V2=18.7	V2=26.3
	n1=0.54	n1=0.64	n1=0.72	n1=0.86
	m1=0.24	m1=0.41	m1=0.60	m1=0.92
	h1=0.16	h1=0.07	h1=0.03	h1=0.01
	n2=0.49	n2=0.55	n2=0.60	n2=0.70
	m2=0.18	m2=0.25	m2=0.34	m2=0.53
	h2=0.23	h2=0.15	h2=0.10	h2=0.04
Type of condition	Hopf	Limit Point	Hopf	Hopf

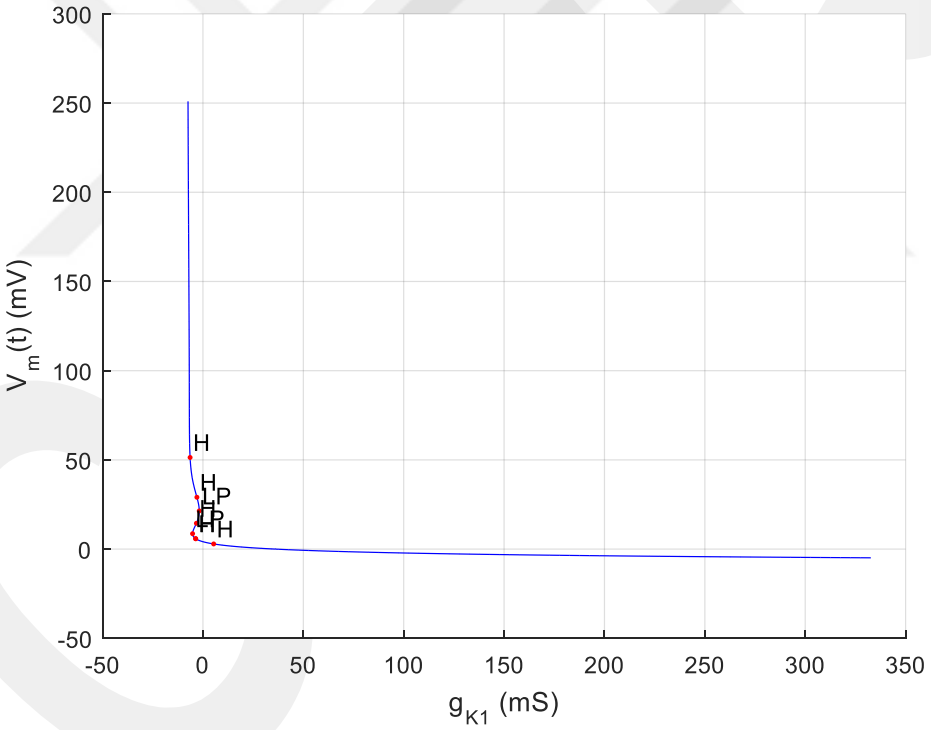

Figure 5. 9 Bifurcation diagram of H-H model against varying parameter gK1 when gc=10 in Table 5.8.

Table 5. 10 Bifurcation analysis results for gna1 when gc = 10

Parameters	gk=36, gna=120, gl=0.3, Vk=-12, Vna=115, Vl=10.6, Cm=0.91	
Equilibrium points	gna1 = 295	
	V1=0.99	
	V2=0.89	
	n1=0.33	
	m1=0.06	
	h1=0.56	
	n2=0.33	
	m2=0.06	
	h2=0.56	
Type of condition	Hopf	

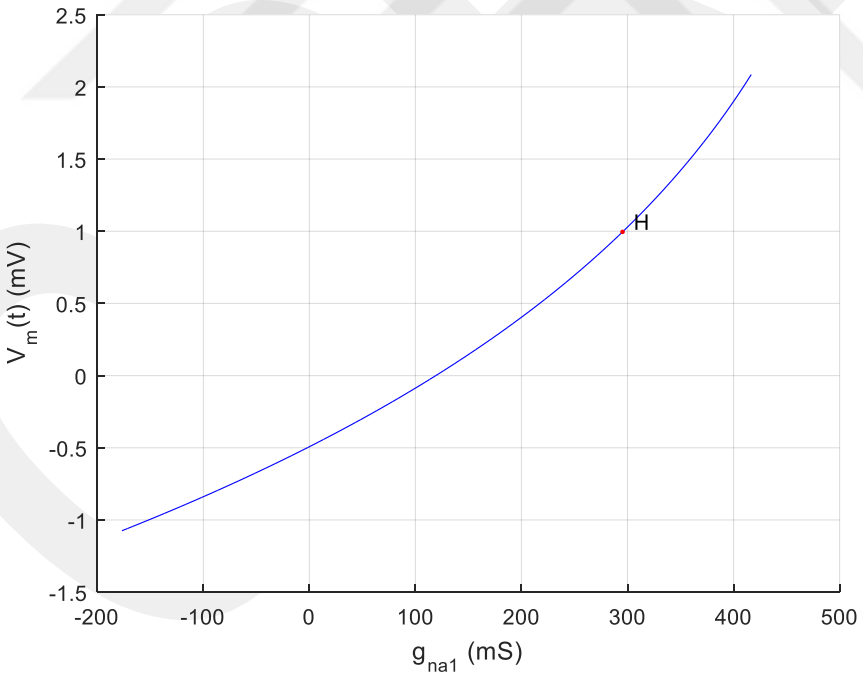

Figure 5. 10 Bifurcation diagram of H-H model against varying parameter gna1when gc=10 in Table 5.10

CHAPTER 6

RESULTS AND SIMULATION

6.1. Washout Filter of Coupled Hodgkin-Huxley Neurons

A washout filter is a high pass filter that rejects steady state inputs, while passing transient inputs. The main benefit of using washout filters is that all the equilibrium points of the open-loop system are preserved (i.e., their location isn't changed).Although washout filters have been successfully used in many control application, there is no systematic way for choosing the constants of the washout filters and the control parameters. The represented form of the washout filter is:

$$G(s) = \frac{Y(s)}{X(s)} = \frac{s}{s+a}$$

$$G(s) * (s + a) = s$$

$$G(s) * s + G(s) * a = s$$

$$G(s) = 1 - \frac{a}{s+a}$$

Here, d is the reciprocal of the filter time constant which is positive for a stable filter and negative for an unstable filter. With the notation

$$z(s) = \frac{1}{s+a}\, x(s)$$

the dynamics of the filter can be written as

$$\dot{z} = x - dz$$

along with the output equation

$$y = x - dz$$

In discrete time, the dynamics of a wash out filter can be written as

$$z(\,k+1\,) = x(k) + (1-d)\,z(k)$$

along with output equation

$$y\,(k) = x(k) - dz(k).$$

For a stable washout filter, the filter constant satisfies $0 < d < 2$.

The high pass filter can be represented in state-space as:

$$\dot{z} = \propto_w z + \beta_w y$$

$$I = \propto_w z + \beta_w y$$

Where

z : State of the washout filter $z \in R^n$

y : Measured output of the system which needs controlling.

I : Output of the washout filter and it is the input (u) to the controlled system $I \in R^n$.

$\propto_w$: State of the system $\propto_w \in R^{r*c}$. r is a raw and c is a column.

β_w : State of the system $\beta_w \in R^r$.

The number of columns in β_w depends on the size of (y). To apply the state feedback control techniques, one must have to augment the washout filter to the original nonlinear system $\propto_w$ must be Hurwitz matrix or stable matrix which mean all eigenvalues of this matrix have negative real part.

The washout filter acts as a high pass filter passes the transient response of the system and prevents passage steady-state part of it. So that, this filter maintains the natural balance of the physical properties of the system and keep the membrane potential at the natural level. It can use the projective control theory to support the design of the washout filter. To make the procedure easier one may apply the Linear Quadratic Regulator approach to get the reference projective output feedback (K_0) which processes the output of the washout filter. It also seems that it has been a satisfactory approach in the Hopf bifurcation casas.

It works to damp the oscillations that happening because of the change of system parameters.

6.1.1 Projective Control Theory

The Projective Control Method [29] which is a linear method is used in the approximates of state feedback. Where the state feedback would be found by whatever method such as (LQR) method or another. One can't retain all the eigenvalues of the state feedback system when using projective control method. but the number of available outputs for feedback determines the number of eigenvalues which is able to retain. Therefore, the optimal control matrix (K_f) which is obtained from the state feedback is the reference for the projective control method.

Assume the system as :

$$\dot{x} = Ax + Bu$$

$$y = Cx$$

Where

x : State of the linear plant ($x \in R^n$).

u : Input of the linear plant ($u \in R^m$).

y : Output which feed the feedback ($y \in R^T$).

A : ($A \in R^{n*n}$).

B : ($B \in R^{n*m}$).

C : Related matrix between the outputs of the plant and the state ($C \in R^{n*r}$). r is the available feedback lines.

The full state feedback control signal defined as:

$$u = -K_f x$$

The gain matrix: ($K_f \in R^{m*n}$) is the matrix which obtained by using (L.Q.R) theory. The closed loop of state feedback is

$$\dot{x} = \left(A - B K_f \right) x$$

The eigen spectrum of closed loop of the state feedback determine as shown below

$$\Lambda = \begin{bmatrix} \lambda 1 & \cdots & 0 \\ \vdots & \ddots & \vdots \\ 0 & \cdots & \lambda n \end{bmatrix}, \; v = [\, v_1 \,,\, v_2 \,,\, \ldots\ldots\ldots \,,\, v_n \,]$$

$$\Lambda = \text{eig}\left(A - B\, K_f \right)$$

Λ : Diagonal eigenvalues matrix.

v : Eigenvectors matrix.

The eigen spectrum equation is

$$\left(A - B\, K_f \right) v = \Lambda v$$

The control signal u obtained

$$u = -\, K_0\, y$$

Where

$$y = Cx$$

So

$$u = -\, K_0\, Cx$$

The closed-loop dynamic of the output feedback can be found as:

$$\dot{x} = (\, A - B\, K_0\, C)\, x$$

$$(\, A - B\, K_0\, C) v_r = v_r \Lambda_r$$

$$\left(A - B\, K_f \right) v_r = (\, A - B\, K_0\, C) v_r$$

From last equation, we can find the relationship between K_f & K_0

$$K_0 = K_f\, v_r\, (\, C v_r)^{-1}$$

The output feedback gain is K_0 .

6.2. Results and Simulation of Coupled Hodgkin-Huxley Neurons.

Synaptic conductor gc=0.3, will exam Hopf and Limit Point bifurcation which obtained from MATCONT Software.

gc=0.3, Label : Hopf, gk1=15.4.
V1=3.29, V2=0.65, n1=0.37, m1=0.078, h1=0.48, n2=0.33, m2=0.06, h2=0.57
Here successfully stabilized and stopped the oscillations and in 50 milliseconds the membrane potentials successfully covered to the true value of equilibrium points.

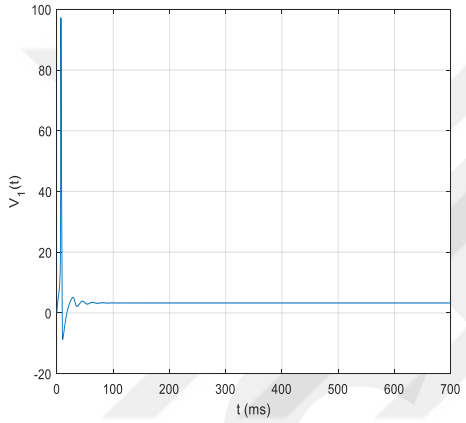

Figure 6. 1 Controlled Variation of V1

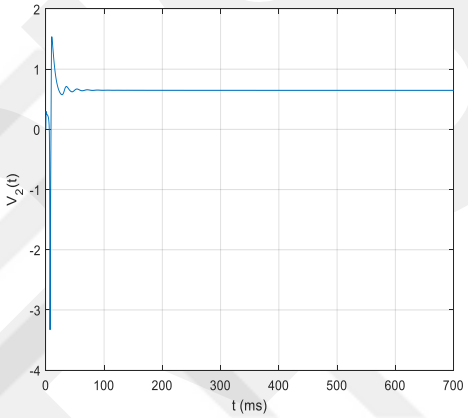

Figure 6. 2 Controlled Variation of V2

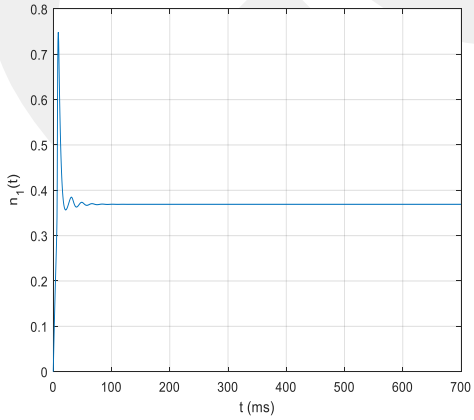

Figure 6. 3 Controlled Variation of n1

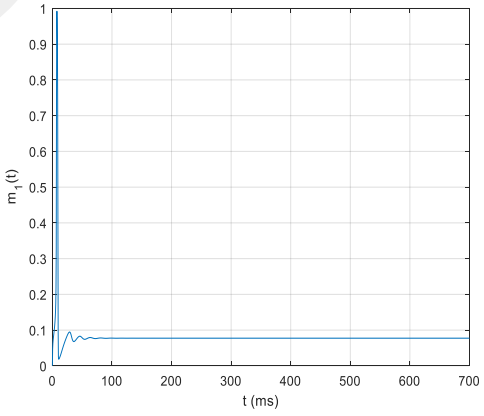

Figure 6. 4 Controlled Variation of m1

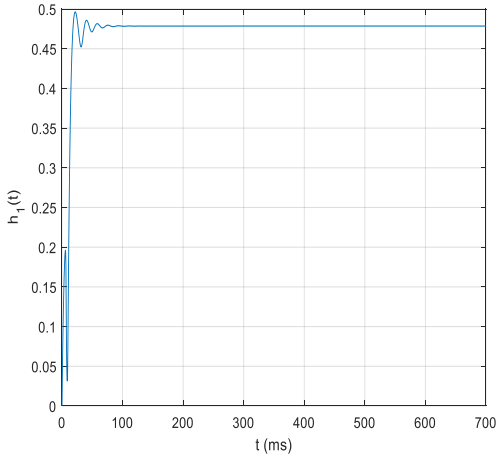

Figure 6. 5 Controlled Variation of h1

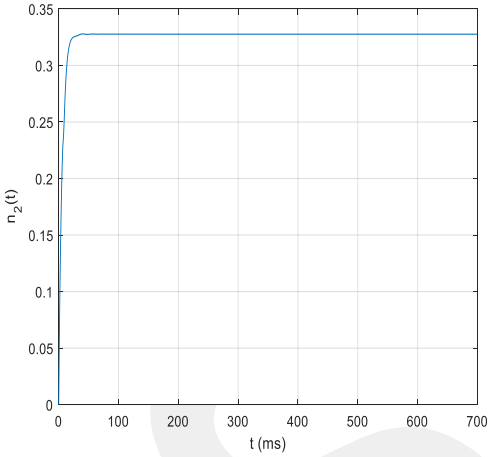

Figure 6. 6 Controlled Variation of n2

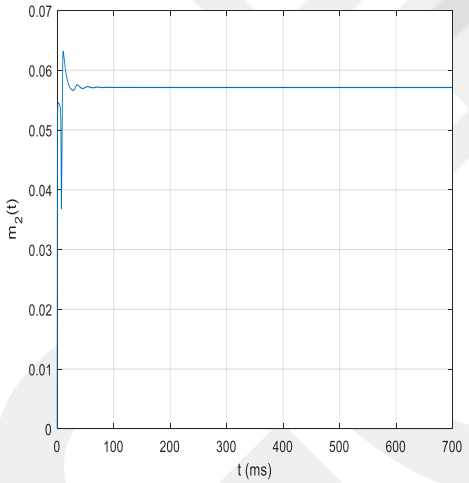

Figure 6. 7 Controlled Variation of m2

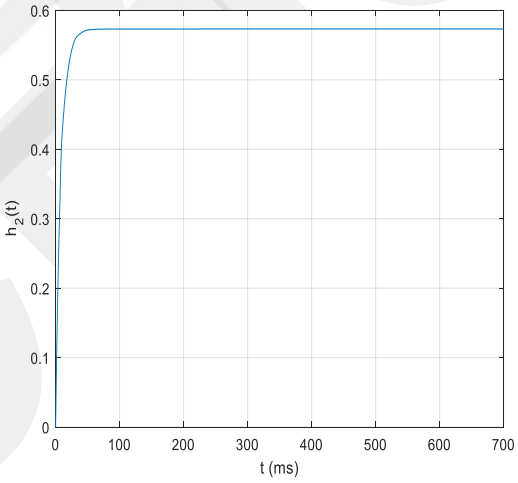

Figure 6. 8 Figure 6.8 Controlled Variation of h2

gc=0.3, Label : Limit Point, gk1=-0.55
V1=102, V2=10.1, n1=0.96, m1=0.99, h1=0.01, n2=0.48, m2=0.16, h2=0.26
stable and stopped the oscillations
The membrane potential takes more time to cover the true value of equilibrium point.

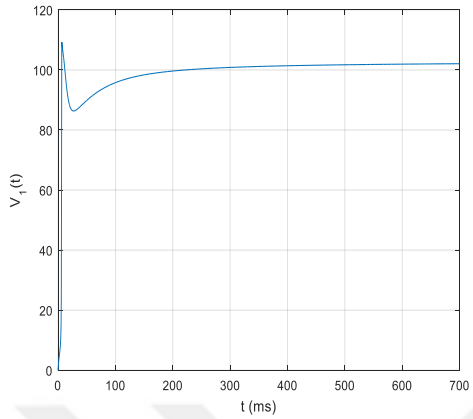

Figure 6. 9 Controlled Variation of V1

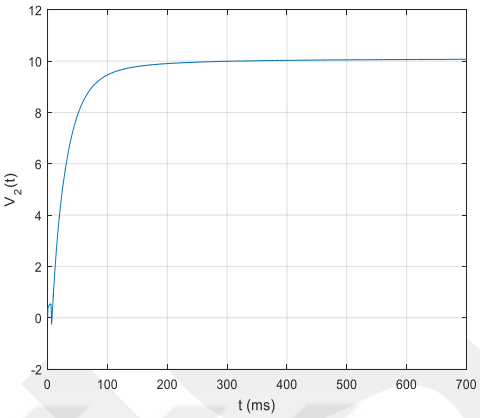

Figure 6. 10 Controlled Variation of V2

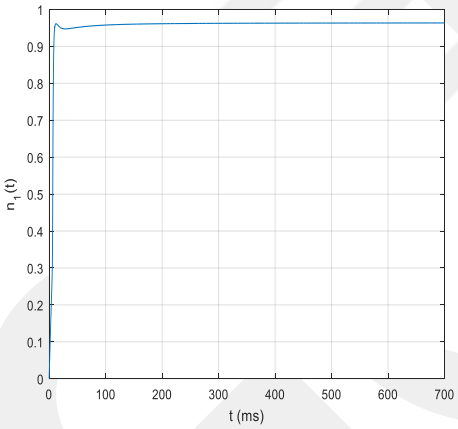

Figure 6. 11 Controlled Variation of n1

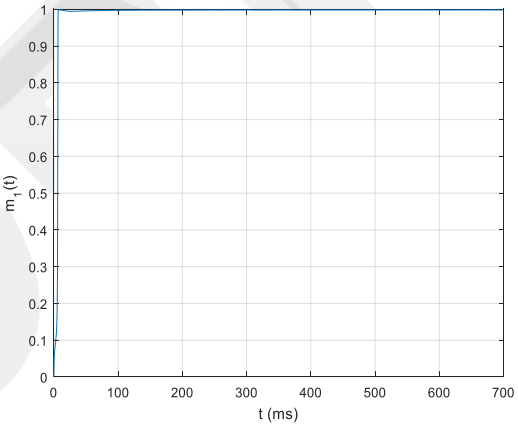

Figure 6. 12 Controlled Variation of m1

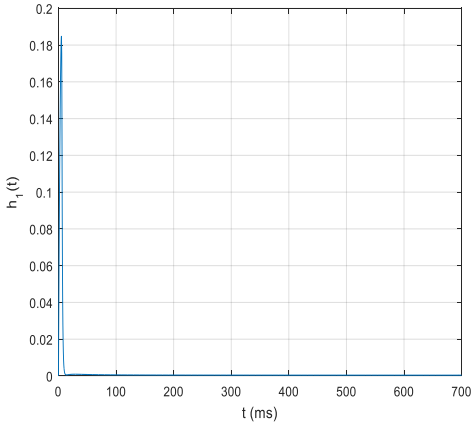

Figure 6. 13 Controlled Variation of h1

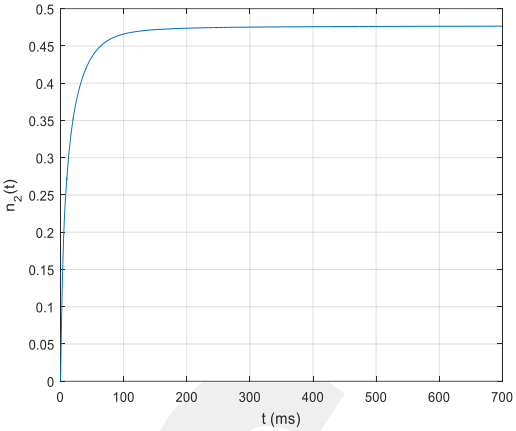

Figure 6. 14 Controlled Variation of n2

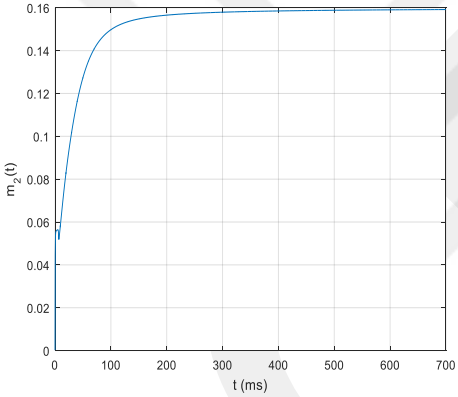

Figure 6. 15 Controlled Variation t of m2

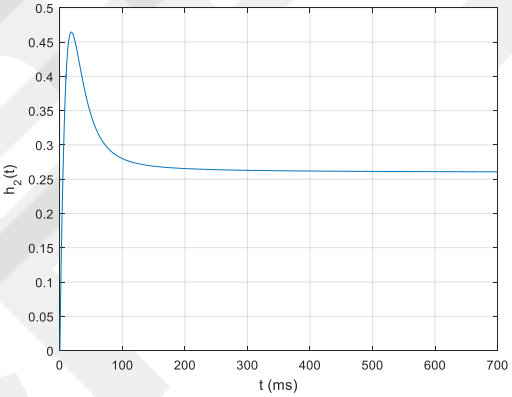

Figure 6. 16 Controlled Variation of h2

gc=0.55, Label = Hopf , gk1=13.4
V1=3.41, V2=1.03, n1=0.37, m1=0.08, h1=0.47, n2=0.33, m2=0.06, h2=0.56

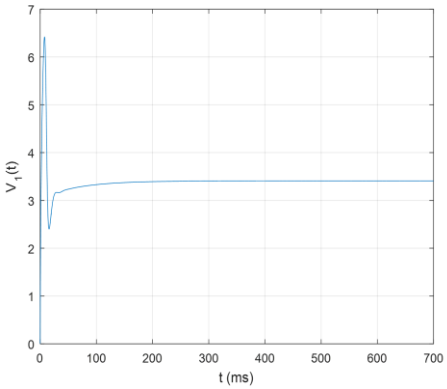

Figure 6. 17 Controlled Variation of V1

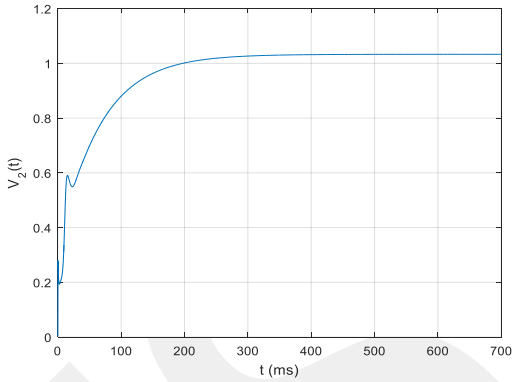

Figure 6. 18 Controlled Variation of V2

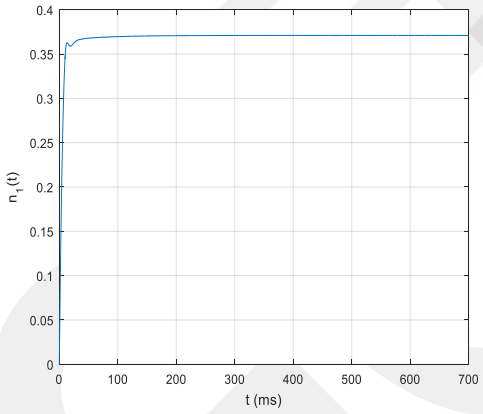

Figure 6. 19 Controlled Variation of n1

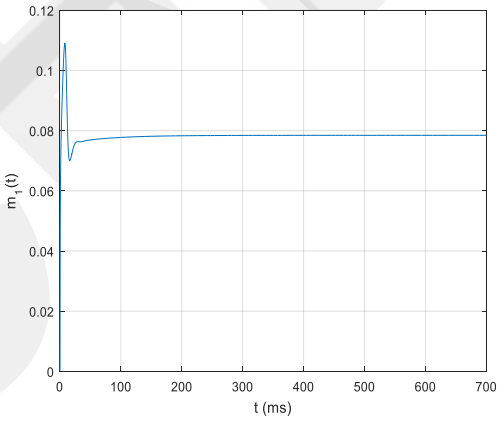

Figure 6. 20 Controlled Variation of m1

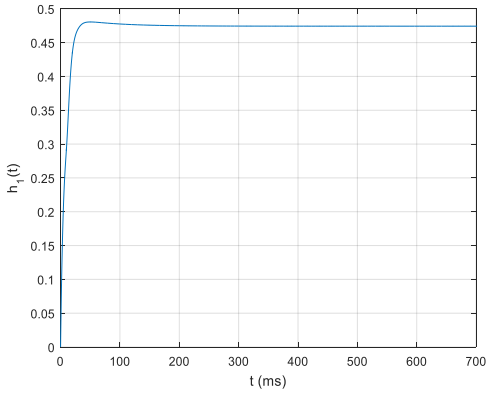

Figure 6. 21 Controlled Variation of h1

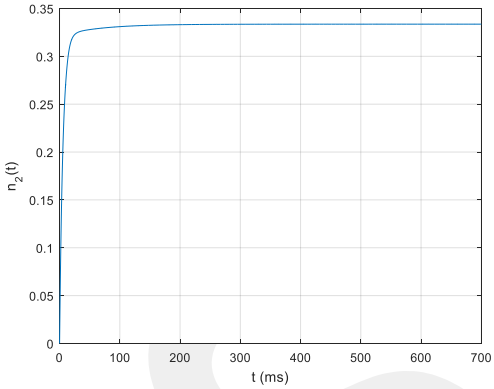

Figure 6. 22 Controlled Variation of n2

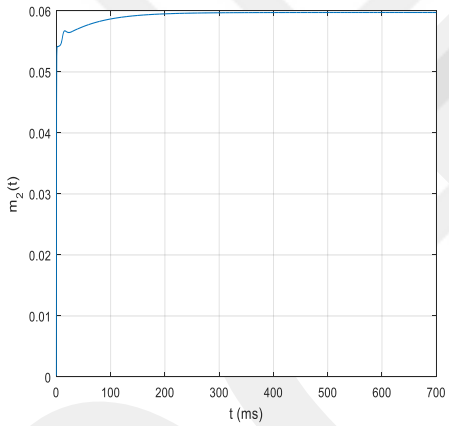

Figure 6. 23 Controlled Variation of m2

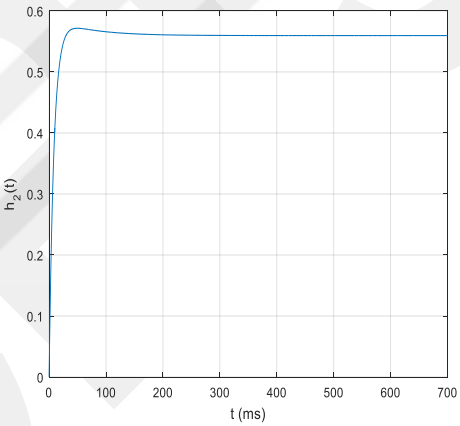

Figure 6. 24 Controlled Variation of h2

gc=0.55, Label = Limit Point, gk1= -0.75
V1=164, V2=16.9, n1=0.99, m1=0.99, h1=0.01, n2=0.58, m2=0.29, h2=0.12

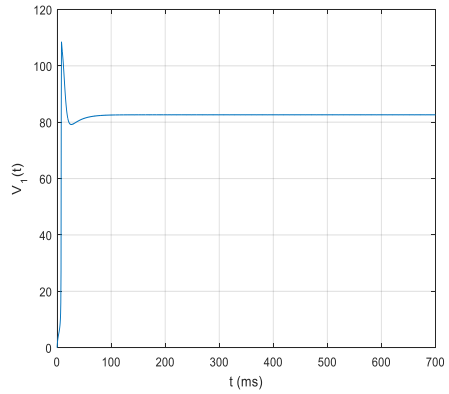

Figure 6. 25 Controlled Variation of V1

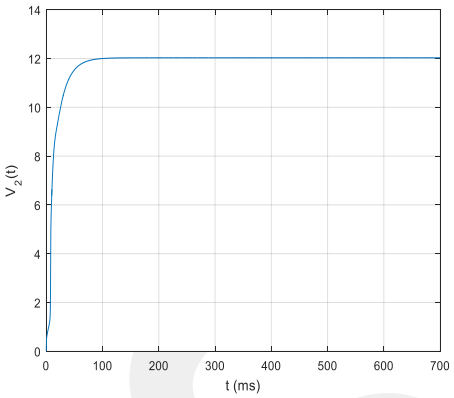

Figure 6. 26 Controlled Variation of V2

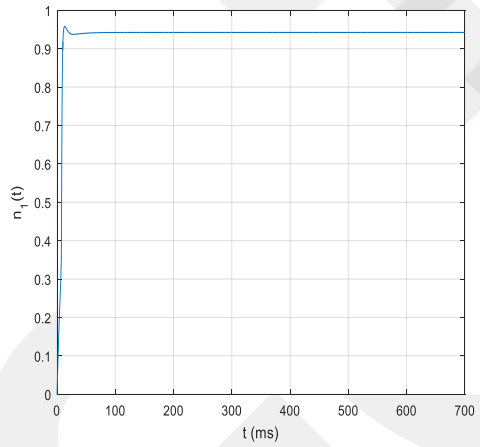

Figure 6. 27 Controlled Variation of n1

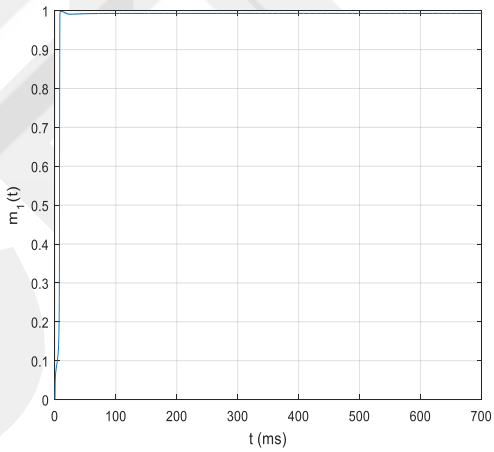

Figure 6. 28 Controlled Variation of m1

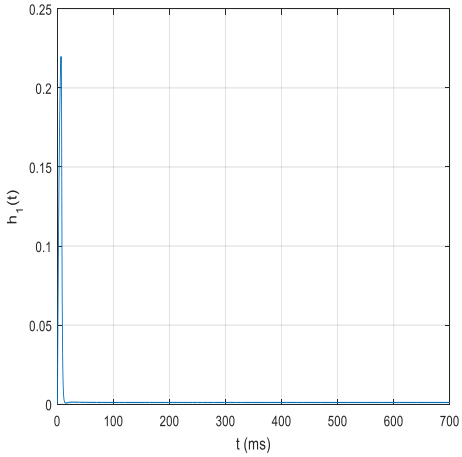

Figure 6. 29 Controlled Variation of h1

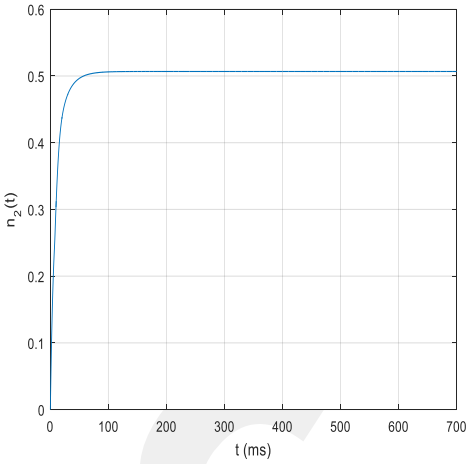

Figure 6. 30 Controlled Variation of n2

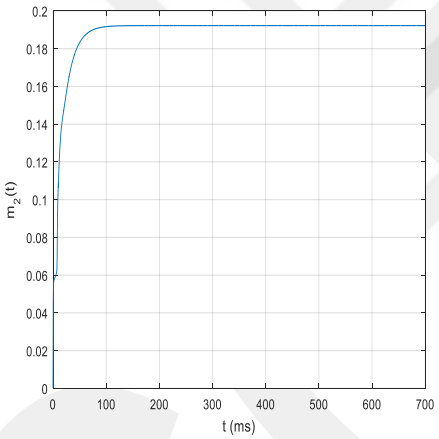

Figure 6. 31 Controlled Variation of m2

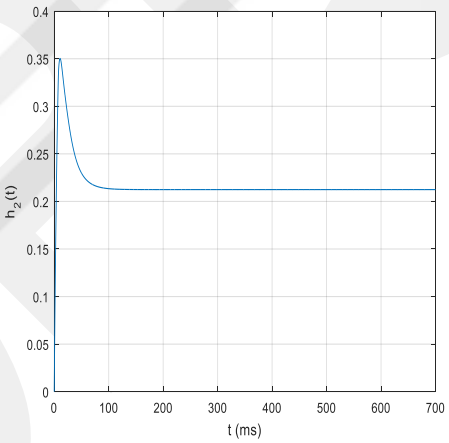

Figure 6. 32 Controlled Variation of h2

gc=1, Label = Hopf , gk1=11.2
V1=3.42, V2=1.48, n1=0.37, m1=0.079, h1=0.47, n2=0.34, m2=0.06, h2=0.54

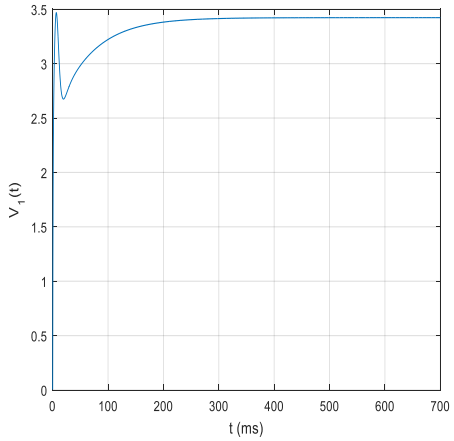

Figure 6. 33 Controlled Variation of V1

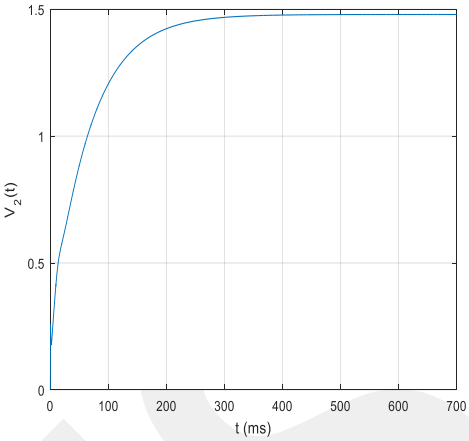

Figure 6. 34 Controlled Variation of V2

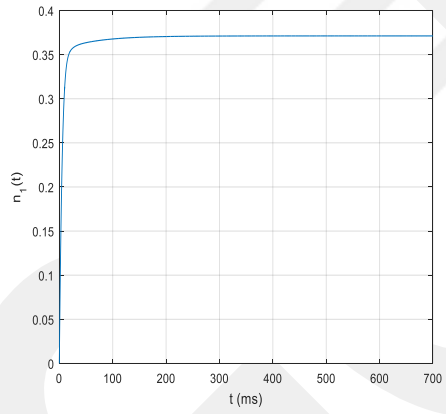

Figure 6. 35 Controlled Variation of n1

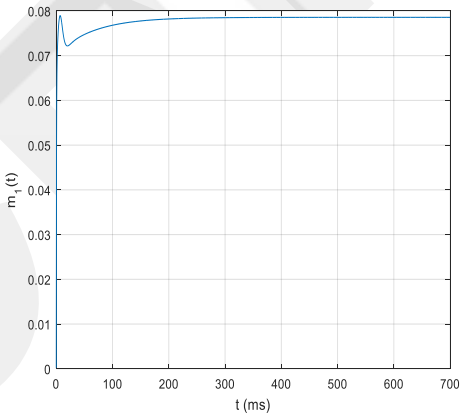

Figure 6. 36 Controlled Variation of m1

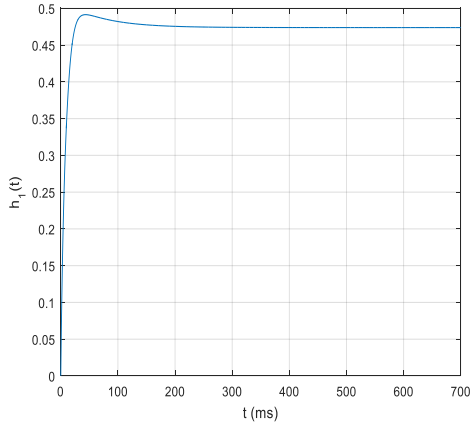

Figure 6. 37 Controlled Variation of h1

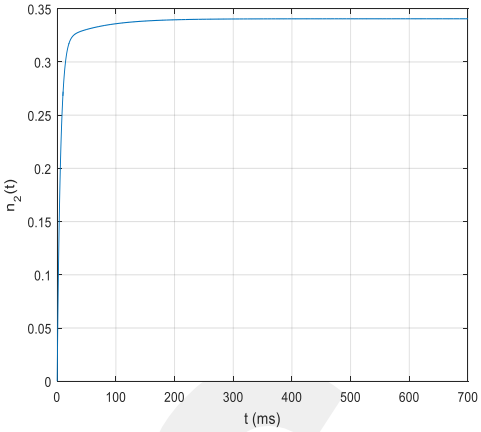

Figure 6. 38 Controlled Variation of n2

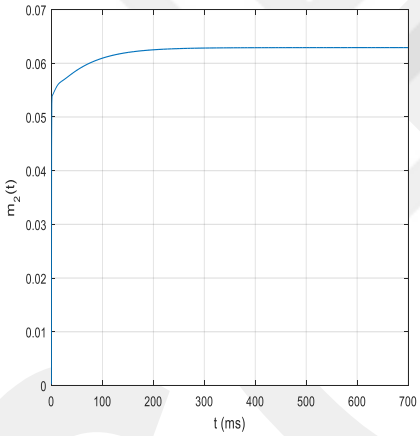

Figure 6. 39 Controlled Variation of m2

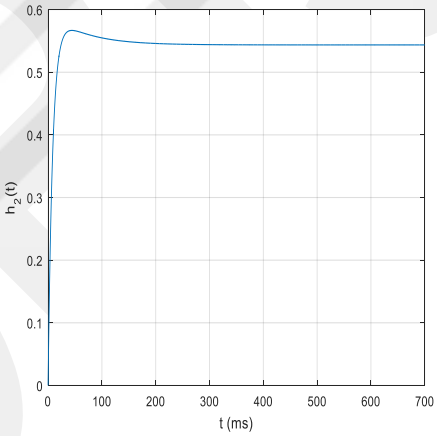

Figure 6. 40 Controlled Variation of h2

gc=1, Label = Limit Point, gk1= -1.14
V1=92.4, V2=16.4, n1=0.95, m1=0.99, h1=0.01, n2=0.57, m2=0.28, h2=0.13

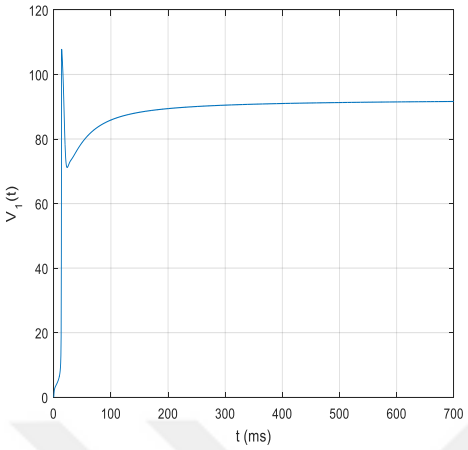

Figure 6. 41 Controlled Variation of V1

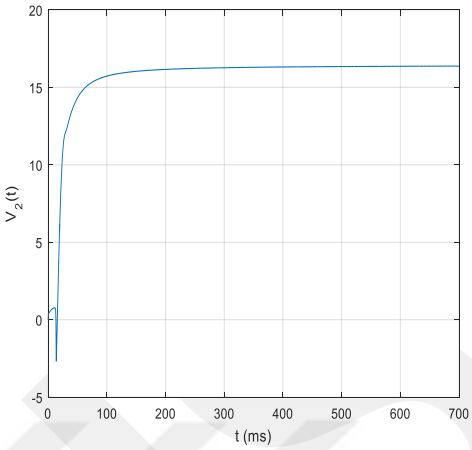

Figure 6. 42 Controlled Variation of V2

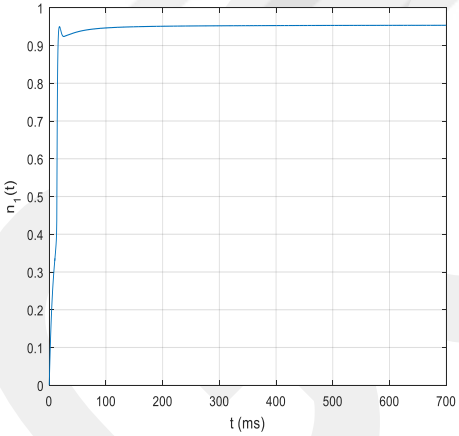

Figure 6. 43 Controlled Variation of n1

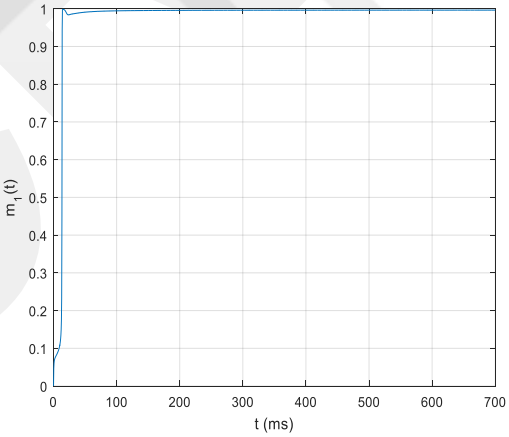

Figure 6. 44 Controlled Variation of m1

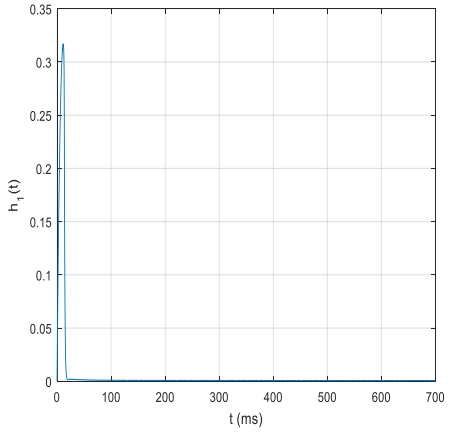

Figure 6. 45 Controlled Variation of h1

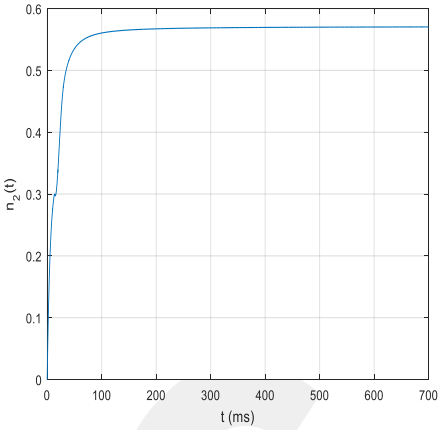

Figure 6. 46 Controlled Variation of n2

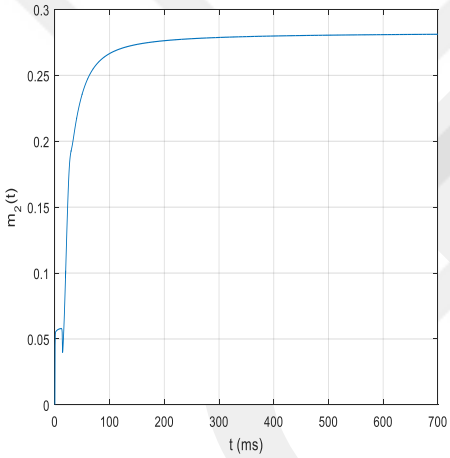

Figure 6. 47 Controlled Variation of m2

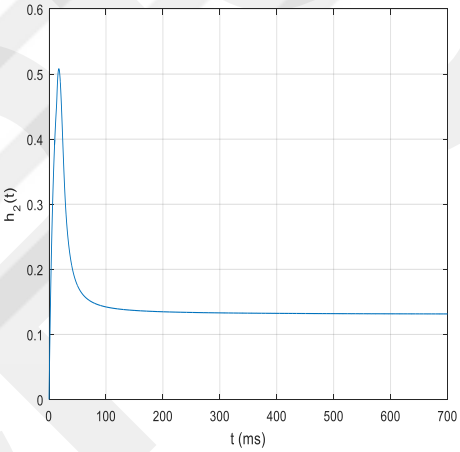

Figure 6. 48 Controlled Variation of h2

gc=10, Label = Hopf, gk1=5.34
V1=2.89, V2=2.52, n1=0.36, m1=0.07, h1=0.49, n2=0.36, m2=0.07, h2=0.51

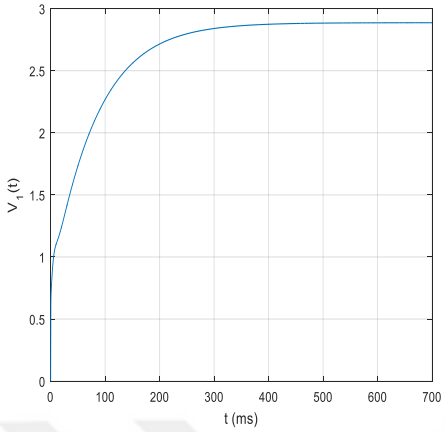

Figure 6. 49 Controlled Variation of V1

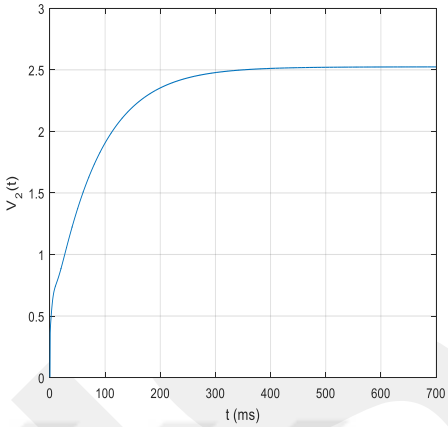

Figure 6. 50 Controlled Variation of V2

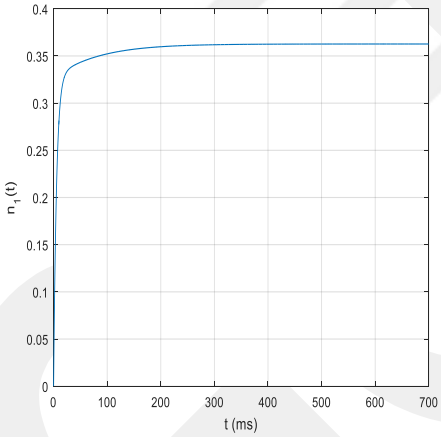

Figure 6. 51 Controlled Variation of n1

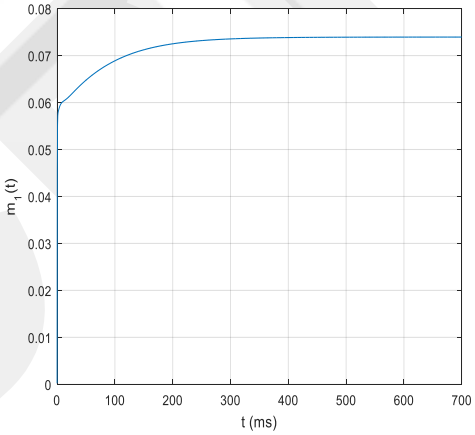

Figure 6. 52 Controlled Variation of m1

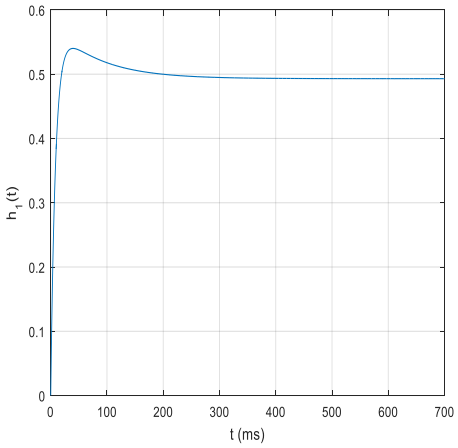

Figure 6. 53 Controlled Variation of h1

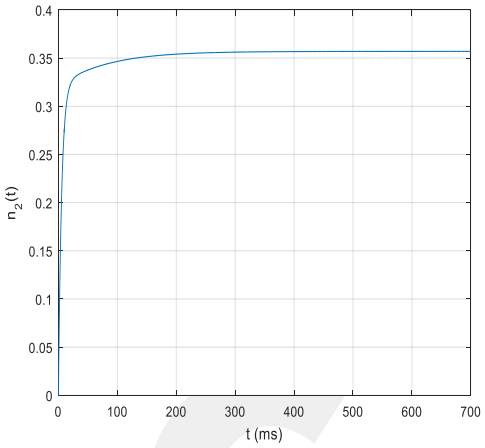

Figure 6. 54 Controlled Variation of n2

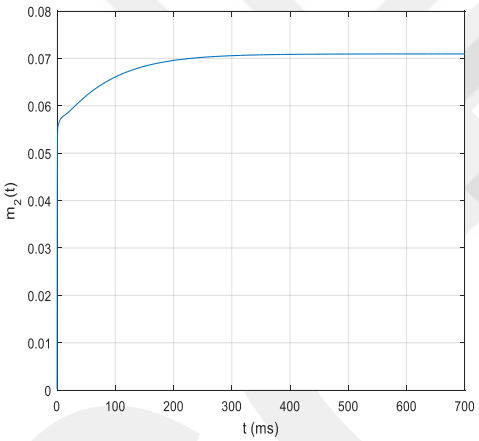

Figure 6. 55 Controlled Variation of m2

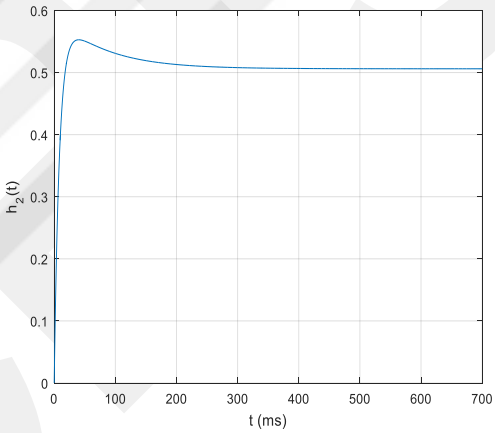

Figure 6. 56 Controlled Variation of h2

CHAPTER 7

CONCLUSION

In this research a method is presented to develop a control algorithm for stabilizing the bifurcations existing in a coupled Hodgkin-Huxley dynamic. The two neurons are coupled by an electrical synaptic conductance. It works to damp the oscillations that are occurring due to a deviation in the system parameters and this problem is being solved by using a second order washout filter. The washout filter acts as a high pass filter and it is expected to be more effective than another control methods because of the fact that it passes the transient response of the system and attenuates the steady-state outputs of the system. So that this filter maintains the natural balance of the physical properties of the system and keeps the membrane potential at its natural level. The study makes use of the projective control theory to support the design of the washout filter. To make the procedure more hassle free we employed a full state feedback linear quadratic regulator to get the reference full state feedback controller that is to be used in the derivation of projective output feedback K_0 which processes the output of the washout filter.

The bifurcations are due to the deviation in the conductance's of the ion channels on the neuron's membrane. To detect all the bifurcations, we first employed the MATCONT software (a free MATLAB toolbox) by [21].

For the Hopf bifurcation, the controller successfully stabilized and stopped the oscillations and the membrane potentials successfully covered to the true value of equilibrium points and the Limit Point bifurcation stable and stopped the oscillations and the membrane potential takes more time to cover the true value of equilibrium points. When lower conductance gc has small values exists a small level of oscillations and when the conductance gc has higher values, it seems much easier to find stable controls.

REFERENCES

[1] A.F. Huxley, F. Andrew, In Squire, Larry R. “The History of Neuroscience in Autobiography”, Washington DC : *Society for Neuroscience*, `1996. pp. 283–318.

[2] M. Edmonds, “http://science.howstuffworks.com/life/inside-the-mind/human-brain/men-women-different-brains1.htm”, Oct. 8, 2008 [Jun. 18, 2017].

[3] A. L Hodgkin, A. F.Huxley, "Action potentials recorded from inside a nerve fibre". *Nature*, vol. 144, pp. 710–711,1939.

[4] R. Fitzhugh, “Thresholds and plateaus in the Hodgkin-Huxley nerve equations”, *The Journal of general physiology*, vol. 43, pp. 867-896, 1960.

[5] "Systems & Control Engineering FAQ in Electrical Engineering and Computer Science, Case Western Reserve University” Internet: engineering.case.edu., Nov. 20, 2015 [Jun. 27, 2017].

[6] B.E. Pfeiffer, K.M.Huber “The state of synapses in fragile X syndrome”. *Neu roscientist*, vol. 15, pp.549-67, Oct 2009.

[7] K.E.Stephan, T. Baldeweg, K. J. Friston “Synaptic plasticity and disconnection in schizophrenia”, *Biol Psychiatry*, vol. 59, pp.929-39, May 2006.

[8] P. Calabresi, B. Picconi, L. Parnetti, M. Di Filippo “A convergent model for cognitive dysfunctions in Parkinson's disease: the critical dopamine-acetylcholine synaptic balance”, *Lancet Neurol*. vol.5, pp. 974-83, Nov 2006.

[9] T.C. Südhof, “Neuroligins and neurexins link synaptic function to cognitive disease”, *Nature*, vol. 455, pp. 903-11, 16 Oct 2008.

[10] D .J. Selkoe ,“Alzheimer's disease is a synaptic failure” *Science*, vol.298, pp. 789-91, 25 Oct 2002;.

[11] J. M. Welch, J. Lu, R.M. Rodriguiz, N. C. Trotta, J. Peca, J.D. Ding, C. Feliciano, M. Chen, J. P. Adams, J. Luo, S. M. Dudek, R. J. Weinberg, N. Calakos, W. C. Wetsel ,G.Feng “Cortico-striatal synaptic defects and OCD-like behaviors in SAPAP3 mutant mice”, *Nature*, vol. 448, pp. 849-900, 2007.

[12] J.A. Kauer, R.C. Malenka, “Synaptic plasticity and addiction”, *Nature Reviews Neuroscience*, vol.8, pp. 844-58, Nov 2007.

[13] J.D. Crawford, Introduction to bifurcation theory, *Reviews of Modern Physics*, vol. 63, pp. 991, 1991.

[14] B.D. Hassard, D.N. Kazarinoff, Y.H. Wan, *Theory and applications of hopf bifurcation*, Cambridge University Press Archive, pp.320, June 1981.

[15] Y. A. Kuznetsov, “Andronov-hopf bifurcation” Scholarpedia, 1(10),

2006.

[16] J.E. Marsden and M. McCracken, “The hopf bifurcation and its applications ”, *Applied Mathematic Science*, vol.19, pp. 424, 1976.

[17] "HOPF-Bifurcations”. (PDF), Department of Mathematics Massachusetts Institute of Technology Cambridge, Massachusetts MA 02139.

[18] E. J. Doedel, A. R. Champneys, T. F. Fairgrieve, Yu. A. Kuznetsov, B. Sandstede, X. J. Wang, “AUTO97: Continuation and Bifurcation Software for Ordinary Differential Equations (with HomCont)”, User’s Guide, Concordia University, Montreal, Canada 1998..

[19] B.D.Hassard, N.D Kazarinoff, Y-H Wan,”Theory and applications of HOPF bifurcation”, *SIAM Review*, 24(4), pp. 498– 499, 1981.

[20] A. Dhooge, W. Govaerts, Y.A. Kuznetsov, “MATCONT: a MATLAB package for numerical bifurcation analysis of ODEs”. *ACM Transactions on Mathematical Software (TOMS)*, vol. 29, pp.141–164, 2003.

[21] J. Rinzel and J. P. Keaner, “Hopf bifurcation to repetitive activity in nerve”, *SIAM Journal on Applied Mathematics*, 43(4), pp.907-922, 1983.

[22] H.Poincaré, "L'Équilibre d'une masse fluide animée d'un mouvement de rotation". *Acta Mathematica*, vol.7, pp. 259-380, Sept 1885.

[23] J. Gao, J. B. Delos, "Quantum manifestations of bifurcations of closed orbits in the photoabsorption spectra of atoms in electric fields". *Phys. Rev.A.*, vol. 56, 1997.

[24] G. Boeing, "Visual Analysis of Nonlinear Dynamical Systems: Chaos, Fractals, Self-Similarity and the Limits of Prediction". *Systems*, 4(4), pp.37-54, 2016.

[25] V. Gintautas, A.W. Hubler "Resonant forcing of nonlinear systems of differential equations.". *Chaos*, Vol. 18, 2008.

[26] Y. A. Kuznetsov, *Elements of Applied Bifurcation Theory*, New York, Springer, 1998.

[27] D. Chen, H.O. Wang, G. Chen, "Anti-control of Hopf bifurcations through washout filters", *Decision and Control, Proceedings of the 37th IEEE conference*, 1998, pp. 3040-3045.

[28] A.L. Hodgkin, A.F.Huxley, "A quantitative description of membrane current and its application to conduction and excitation in nerve". *The Journal of Physiology*, vol.117, pp.500-544, 1952.

[29] K. Wise, F. Deylami, "Approximating a linear quadratic missile autopilot design using an output feedback projective control", AIAA Guidance, *Navigation and Control Conference*, 1991, pp.2613,.

[30] R.Ö. Doruk, "Washout filter based control for the Hodgkin-Huxley nerve cell dynamics". *Turkish Journal of Electrical Engineering & Computer Sciences*, vol.18, pp.553–570, 2010.

[31] R.O. Doruk, "Feedback controlled electrical nerve stimulation: A computer simulation". *Computer Methods and Programs in Biomedicine*, vol.99, pp. 98–112, 2010.

[32] R.Ö. Doruk, "Development of a computer algorithm for feedback controlled electrical nerve fiber stimulation". *Computer Methods and Programs in Biomedicine*, vol.103, pp. 132–144, 2011.

[33] M.E. Nelson, *Electrophysiological Models In: Databasing the Brain: From Data to Knowledge*, New York, Wiley, 2004.

[34] M. Nucci, P. Clarkson, "The nonclassical method is more general than the direct method for symmetry reductions: an example of the fitzhugh-nagumo equation," *Physics Letters A*, 164(1), pp. 49-56, 1992.

[35] A.O. Abdallh, "Control of Bifurcation in Coupled Fitzhugh-Nagumo Neurons", Master Thesis, Atılım University, Turkey, November 2017.

APPENDICES

A. Simulation Program

```
cc
format long g
xi=[3.290680 0.648322 0.369081 0.077405 0.478523 0.327657 0.057121
0.573281];
v1 = xi(1);
v2 = xi(2);
n1 = xi(3);
m1 = xi(4);
h1 = xi(5);
n2 = xi(6);
m2 = xi(7);
h2 = xi(8);
gk1=15.433330;
gna1=120;
gl1=0.3;
vk1=-12;
vna1=115;
vl1=10.613;
cm1=0.91;
gk2=36;
gna2=120;
gl2=0.3;
vk2=-12;
vna2=115;
vl2=10.613;
cm2=0.91;
gc=0.3;
```

```
A=[-(gna1*h1*m1^3 + gk1*n1^4 + gc + gl1)/cm1, gc/cm1, -(4*gk1*n1^3*(v1 -
vk1))/cm1, -(3*gna1*h1*m1^2*(v1 - vna1))/cm1, -(gna1*m1^3*(v1 -vna1))/cm1, 0,

0, 0, gc/cm2,-(gna2*h2*m2^3 + gk2*n2^4 + gc + gl2)/cm2,0, 0,0, -(4*gk2*n2^3*(v2
- vk2))/cm2,-(3*gna2*h2*m2^2*(v2 - vna2))/cm2, -(gna2*m2^3*(v2 -vna2))/cm2

(n1*exp(-v1/80))/640 + (n1 - 1)/(100*(exp(1 - v1/10) - 1)) + (exp(1- v1/10)*(v1/100
- 1/10)*(n1 - 1))/(10*(exp(1 - v1/10) - 1)^2),0, (v1/100 - 1/10)/(exp(1 - v1/10) - 1) -
exp(-v1/80)/8,0, 0,0, 0,0(2*m1*exp(-v1/18))/9 + (m1 - 1)/(10*(exp(5/2 - v1/10) - 1))
+(exp(5/2 - v1/10)*(v1/10 - 5/2)*(m1 - 1))/(10*(exp(5/2 - v1/10) -1)^2),0, 0, (v1/10 -
5/2)/(exp(5/2 - v1/10) - 1) - 4*exp(-v1/18),0, 0,0, 0(7*exp(-v1/20)*(h1 - 1))/2000 -
(h1*exp(3 - v1/10))/(10*(exp(3 -v1/10) + 1)^2),0, 0,0, - (7*exp(-v1/20))/100 -
1/(exp(3 - v1/10) + 1),0, 0,0,0, (n2*exp(-v2/80))/640 + (n2 - 1)/(100*(exp(1 - v2/10)
- 1)) +(exp(1 - v2/10)*(v2/100 - 1/10)*(n2 - 1))/(10*(exp(1 - v2/10) - 1)^2),0, 0,0,
(v2/100 - 1/10)/(exp(1 - v2/10) - 1) - exp(-v2/80)/8,0, 0,0, (2*m2*exp(-v2/18))/9 +
(m2 - 1)/(10*(exp(5/2 - v2/10) - 1)) +(exp(5/2 - v2/10)*(v2/10 - 5/2)*(m2 -
1))/(10*(exp(5/2 - v2/10) -1)^2), 0,0, 0,0, (v2/10 - 5/2)/(exp(5/2 - v2/10) - 1) -
4*exp(-v2/18),0,0, (7*exp(-v2/20)*(h2 - 1))/2000 - (h2*exp(3 - v2/10))/(10*(exp(3 -
v2/10) +1)^2), 0,0, 0,0, 0, - (7*exp(-v2/20))/100 - 1/(exp(3 - v2/10) + )];

B=[01/cm2,0 0 0 0 0 0];

aw1=-0.1;

bw1=1;

aw2=-0.1;

bw2=1;

Cw=[bw1 0 0 0 0 0 0 0 aw1 0

0 bw2 0 0 0 0 0 0 0 aw2];

Aw=[A zeros(8,2);Cw];

Bw=[B;0;0];

Q=100*eye(10); % Order of A+ 1 for 1st order washout filter.

R=1;

K=lqr(Aw,Bw,Q,R);

[hh_vecs,hh_vals]=eig(Aw-Bw*K);

hh_eig=eig(Aw-Bw*K);

[hh_eig_sorted,ndx]=esort(hh_eig); % You need to choose the retained eigenvalues
from this list.

hh_eig_sorted % You can see the list of eigenvalues from this list.

% PLEASE NOTE: The number of eigenvalues that can be retained equals to the
order of the washout filter as it is applied in the projective control procedure. The
problem is that you will not be able to retain the complex eigenvalues when you have
a first order washout filter. So do not % try to retain the first two eigenvalues.
Complex eigenvalues should always be retained as pairs as they appear as complex
```

conjugates. Otherweise we will have unreal coefficients which have no physical meaning.

V5=hh_vecs(:,ndx(9:10)); % To retain the 3rd eigenvalue.

Ks=K*V5*inv(Cw*V5)

Ksr=real(Ks)

hh_eig_pro=eig(Aw-Bw*Ksr*Cw);

hh_eig_pro

B. Design Program

```
clear
close all
global cds
%assign parameter values
gkm=36;
gnam=120;
glm=0.3;
vk=-12;
vna=115;
vl=10.613;
cmm=0.91;
cm1=cmm;
cm2=cmm;
gc=0.3;
gk1=gkm;
gk2=gkm;
gl1=glm;
gl2=glm;
gna1=gnam;
gna2=gnam;
vk1=vk;
vk2=vk;
vl1=vl;
vl2=vl;
vna1=vna;
vna2=vna;
u1=0;
u2=0;
init;
p=[cm1 cm2 gk1 gk2 gna1 gna2 gl1 gl2 vk1 vk2 vna1 vna2 vl1 vl2 gc u1
u2];
ap=3;
opt=contset;opt=contset(opt,'MaxNumPoints',10000);
opt=contset(opt,'MaxCorrIters',1000);
opt=contset(opt,'MaxNewtonIters',1000);
opt=contset(opt,'MaxTestIters',1000);
opt=contset(opt,'Singularities',1);
opt=contset(opt,'MaxNumPoints',3000);
opt=contset(opt,'CheckClosed',500);
opt=contset(opt,'MinStepSize',1e-3);
opt=contset(opt,'InitStepSize',1e-5);
opt=contset(opt,'MaxStepSize',1e-1);
XEQ=[0.00362066888179067
       0.00362066883437867
         0.317732399761838
        0.0529550868134409
         0.595994124737657
```

```
          0.317732399761276
         0.0529550868131441
          0.595994124739102];
[x0,v0]=init_EP_EP(@ab_hh2test, XEQ , p, ap);
[x,v,s,h1,f1]=cont(@equilibrium,x0,[],opt);
%[x,v,s,h1,f1]=cont(x,v,s,h1,f1,cds);
%[x,v,s,h1,f1]=cont(x,v,s,h1,f1,cds);
%[x,v,s,h1,f1]=cont(x,v,s,h1,f1,cds);
```